Available online at www.sciencedirect.com

SciVerse ScienceDirect

Geochimica et Cosmochimica Acta 101 (2013) 57–75

Geochimica et Cosmochimica Acta

www.elsevier.com/locate/gca

Modern soil system constraints on reconstructing deep-time atmospheric CO_2

Isabel P. Montañez *

Department of Geology, University of California, Earth and Physical Sciences Bldg., One Shields Drive, Davis, CA 95616, USA

Received 3 May 2012; accepted in revised form 6 October 2012; Available online 22 October 2012

Abstract

Paleosol carbonate-based estimates of paleo-atmospheric CO_2 play a prominent role in constraining radiative-forcing and climate sensitivity in the deep-time. Large uncertainty in paleo-CO_2 estimates made using the paleosol-carbonate CO_2-barometer, however, arises primarily from their sensitivity to soil-respired CO_2 ($S(z)$). This parameter is poorly constrained due to a paucity of soil CO_2 measurements during carbonate formation in modern soils and a lack of widely applicable proxies of paleo-soil CO_2. Here the $\delta^{13}C$ values of carbonate and soil organic matter (SOM) pairs from 130 Holocene soils are applied to a two-component CO_2-mixing equation to define soil order-specific ranges of soil CO_2 applicable for constraining $S(z)$ in their corresponding paleosol analogs.

Equilibrium carbonate–SOM pairs, characterized by $\Delta^{13}C_{carb-SOM}$ values of 12.2–15.8‰, define a mean effective fractionation of 14.1‰ and overall inferred total soil CO_2 contents during calcite formation of <1000–10,000 ppmv. For those Aridisols and Alfisols, characterized by a net soil-moisture deficit, and their paleosol analogs (Calcisols and Argillisols), a best estimate of $S(z)$ during calcite formation is 1500–2000 ppmv (range of 500–2500 ppmv). Overall higher values (2000–5000 ppmv) are indicated by the subset of these soils characterized by higher moisture content and productivity. Near atmospheric levels (400 ± 200 ppmv) of estimated $S(z)$ are indicated by immature soils, recording their low soil productivity. Vertisols define the largest range in total soil CO_2 (<1000 to >25,000 ppmv) reflecting their seasonally driven dynamic hydrochemistry. A $S(z)$ range of 1000–10,000 ppmv is suggested for paleo-Vertisols for which calcite precipitation can be constrained to have occurred in an open system with two-component CO_2 mixing, with a best estimate of 2000 ppmv ± 1000 ppmv appropriate for paleo-Vertisols for which evidence of protracted water saturation is lacking. Mollisol pairs define a best estimate of $S(z)$ of 2500 ppmv (range of 600–4000 ppmv) for late Cretaceous and Cenozoic analogs.

Non-equilibrium pairs with $\Delta^{13}C$ values >16‰ make up 51% of the dataset, lending support to the hypothesis that pedogenic carbonate precipitation occurs during periods of low productivity in a soil atmosphere with a large component of atmospheric CO_2. Predictable scaling between estimated soil CO_2 and the difference in $\delta^{13}C$ between measured pedogenic carbonate and that predicted to have formed from soil-respired CO_2 (inferred from measured SOM) can be used to further constrain appropriate ranges of $S(z)$ for reconstruction of paleo-atmospheric pCO_2. Soil CO_2 estimates are poorly correlated to mean annual precipitation likely reflecting that for carbonate-bearing soils, where moisture limits CO_2 production, total soil CO_2 is most strongly influenced by actual evapotranspiration.

1. INTRODUCTION

Atmospheric pCO_2 is currently 35% higher than concentrations during the past 800 ky and well within the range reconstructed for the last known period of sustained global warming ~3 my ago (Early Pliocene) (NRC, 2011). With

* Tel.: +1 530 754 7823; fax: +1 530 752 0951.
E-mail address: ipmontanez@ucdavis.edu.

0016-7037/$ - see front matter © 2012 Elsevier Ltd. All rights reserved.
http://dx.doi.org/10.1016/j.gca.2012.10.012

the current rate of carbon emissions to the atmosphere, CO_2 is projected to rise within this century to a level last experienced prior to the onset of our current glacial state, and potentially within the next few centuries, to pre-Cenozoic values (Beerling and Royer, 2011; NRC, 2011; Kidder and Worsley, 2012). Earth's temperature response to such CO_2-forcing depends on its climate sensitivity, defined as the change in mean global surface temperature after a doubling of CO_2. Climate sensitivity estimates, however, vary over an order of magnitude (IPCC, 2007; Knutti and Hegerl, 2008; Haywood et al., 2011), reflecting not only their associated uncertainty but also that this sensitivity likely evolves with magnitude and longevity of CO_2-forcing (Hansen et al., 2008).

Constraining change in atmospheric CO_2 content and climate sensitivity beyond the continental ice record (Siegenthaler et al., 2005) is based on mass balance models of sedimentary carbon and sulfur (Berner, 1997, 2006) and plant- and mineral-based proxies (reviewed in NRC, 2011; Royer et al., 2001). The paleosol-carbonate CO_2-barometer (Cerling, 1991) has become the most widely applied method for estimating paleo-atmospheric CO_2 contents (e.g., Mora et al., 1996; Ekart et al., 1999; Driese et al., 2000; Ghosh et al., 2001; Tanner et al., 2001; Nordt et al., 2002; Robinson et al., 2002; Nordt, 2003; Prochnow et al., 2006; Montañez et al., 2007; Cleveland et al., 2008; Retallack, 2009; Schaller et al., 2011). The dependence on paleosol-based CO_2 estimates is greatest for past periods for which higher precision CO_2 proxies (e.g., fossil leaf stomatal frequency, foraminiferal boron isotopes, phytoplankton $\delta^{13}C$) are lacking and for periods of high pCO_2 when biologic proxies saturate (NRC, 2011; Royer et al., 2001).

Estimates of paleo-atmospheric CO_2 made using the paleosol-carbonate CO_2-barometer, however, are associated with large uncertainty (several 100s to 1000s ppmv) compromising the ability to evaluate the role of CO_2-forcing during past periods of major environmental perturbation (Veizer et al., 1999; Beerling and Royer, 2011; NRC, 2011; Honisch et al., 2012). The largest source of uncertainty in the accuracy and precision of CO_2 estimates is their sensitivity to the model input parameter, soil-respired CO_2 (Ekart et al., 1999). A paucity of soil CO_2 measurements during carbonate formation in modern soils and of proxies of paleo-soil CO_2 has made this parameter challenging to constrain. Defining soil-respired CO_2 values applicable to the range of different paleosol types found in the geologic record and that are analogous to many of the modern soil orders (Soil Survey Staff, 2010), ultimately awaits field calibration studies of modern soils such as recently carried out in New Mexico (Breecker et al., 2009), and currently underway in soils of the Texas Coastal Plain (Breecker et al., in press).

In this study, the C isotopic values of pedogenic carbonates and their corresponding organic matter from an extensive suite of Holocene soils that represent six of the 12 soil orders and a range of climate regimes are applied to a two-component CO_2-mixing model to define soil order-specific ranges of soil CO_2. This compilation of C isotope and climate parameters is further used to (1) evaluate recently proposed soil-respired CO_2 proxies developed using climate-soil CO_2 relationships in modern carbonate-bearing soils, and (2) to assess the utility of $\delta^{13}C_{carb}$ and $\delta^{13}C_{SOM}$ in paleosols as a metric of paleo-soil productivity that can be used to further constrain appropriate values of soil-respired CO_2 for the paleo-CO_2 barometer model.

2. THE PALEOSOL-CARBONATE CO_2-BAROMETER

Calcite precipitates in soils under sub-humid to arid climates characterized by a range of precipitation levels and moderate to high evapotranspiration (Machette, 1985; Buol et al., 2003; Soil Survey Staff, 2010). The CO_2 in the soil atmosphere, which is the primary contributor to the C isotopic composition of pedogenic carbonate ($\delta^{13}C_{carb}$), is derived from one or more sources (Sheldon and Tabor, 2009). In well-drained soils characterized by open system gas exchange between the soil atmosphere and free air, the CO_2 is derived from two sources: (1) the atmosphere and (2) a biologically respired source provided by *in situ* microbial oxidation of soil organic matter (SOM) and root respiration. For such soils, $\delta^{13}C_{carb}$, if formed in isotopic equilibrium with soil CO_2, can be applied to a two-component C isotope-mixing model to estimate atmospheric pCO_2 given the two isotopically distinct sources of C (Cerling, 1984, 1991). Soils, however, can be characterized by a single component of CO_2 (e.g., water-saturated soils) or by mixing of three components of CO_2 (an additional host limestone or detrital or eolian $CaCO_3$ source) rendering them inappropriate for application to the paleosol-carbonate CO_2-barometer (see Section 3.1 for further discussion).

This mixing model (Cerling, 1991, 1999), is described by the equation:

$$[CO_2]_{atm} = S(z)\frac{\delta^{13}C_s - 1.0044\delta^{13}C_r - 4.4}{\delta^{13}C_a - \delta^{13}C_s} \quad (1)$$

where the multiplier $S(z)$ is the soil-derived (respired) component of total CO_2 (ppmv) at depth z, $\delta^{13}C_{s,r,a}$ are the C isotopic compositions of total soil CO_2, soil-respired CO_2, and the atmosphere, respectively. $\delta^{13}C_s$ is inferred from $\delta^{13}C$ of calcite nodules, rhizoliths or calcite pendants on clasts, whereas $\delta^{13}C_r$ is inferred from the $\delta^{13}C$ of SOM extracted from the paleosol matrix or occluded within pedogenic carbonates, or from associated fossil leaf cuticle. $\delta^{13}C_a$ is inferred from the $\delta^{13}C$ values of contemporaneous marine biogenic calcites or fossil leaves assuming appropriate equilibrium isotopic fractionations (e.g., Ekart et al., 1999; Montañez et al., 2007; Retallack, 2009). The numeric coefficient and constant account for the difference in diffusivity between $^{13}CO_2$ and $^{12}CO_2$.

CO_2 estimates obtained using the paleosol carbonate CO_2 barometer are most sensitive to the multiplier $S(z)$ compromising their accuracy and precision by potentially several 100–1000s of ppmv (Fig. 1). Uncertainty in the inferred temperature of carbonate precipitation and of contemporaneous atmospheric $\delta^{13}C$ further limit the accuracy and precision of estimates, but typically by well less than half that defined by the uncertainty in $S(z)$ (Fig. 1).

The $S(z)$ parameter cannot be directly measured in ancient soils and there is no quantitative proxy for total soil CO_2 yet demonstrated to be reliable for all paleosols (e.g.,

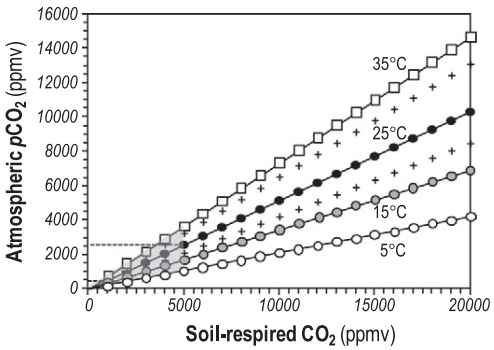

Fig. 1. Sensitivity of the paleosol-carbonate CO_2-barometer to variation in soil-respired CO_2 ($S(z)$), temperature, and $\delta^{13}C_{atm}$. Range of $S(z)$ and temperatures shown are representative of those (total soil CO_2-300 ppmv), reported for carbonate-forming soils (see text for references). Over the $S(z)$ range (1000–5000 ppmv) utilized in previous paleo-atmospheric CO_2 reconstructions, and for a given temperature (25 °C, black-filled circles) and $\delta^{13}C_{atm}$ (−6.5‰), atmospheric CO_2 estimates vary between 300 and 2500 ppmv (dashed horizontal lines). Over the same $S(z)$ range and maximum likely span of carbonate precipitation temperatures (5–35 °C), atmospheric CO_2 estimates vary by 500 ppmv at low $S(z)$ to 2500 ppmv for the higher limit (shaded area). Given that precipitation temperature can typically be constrained to within ±5–10 °C for paleosols for which the paleolatitude and paleoclimate regime are constrained, the impact of temperature uncertainty on CO_2 estimates is likely well less than half that associated with uncertainty in $S(z)$. Varying $\delta^{13}C_{atm}$ by ±2‰ (crosses) for a constant temperature (25 °C) and the aforementioned $S(z)$ range yields atmospheric CO_2 estimates that differ by 100 (low $S(z)$) to 1100 ppmv (high $S(z)$). Variation in $\delta^{13}C_{atm}$ of ±2‰ captures the uncertainty associated with C isotope fractionation factors for C3 plants-atm. CO_2 (Arens et al., 2000; Gröcke, 2002) and $CO_{2(g)}$–calcite (Romanek et al., 1992; Zhang et al., 1995), and accounts for the observed variability, at any given time, in ambient seawater $\delta^{13}C$ inferred from open ocean or epeiric sea proxy data (e.g., Grossman et al., 2008; Prokoph et al., 2008).

Retallack, 2009; Sheldon and Tabor, 2009; Cotton and Sheldon, 2012). Past studies have either applied a constant $S(z)$ value (between 3000 and 6000 ppmv) in order to minimize the large effect of this parameter on CO_2 estimates (e.g., Mora et al., 1996; Ekart et al., 1999; Nordt et al., 2002, 2006; Nordt, 2003; Prochnow et al., 2006; Schaller et al., 2011) or used a range of values defined broadly for modern soil analogs (Montañez et al., 2007). Soil CO_2 contents, however, can vary by two orders of magnitude (Amundson and Davidson, 1990), with some tropical rain forest soils reaching CO_2 levels of several 10^5 ppmv (Brook et al., 1983; Matsumoto et al., 1997). Well-drained carbonate-bearing soils, however, are typically associated with low to moderate productivity leading to soil CO_2 concentrations between 1000 and 10,000 ppmv (Brook et al., 1983; Soloman and Cerling, 1987; Quade et al., 1989; Serna-Perez et al., 2006; Breecker et al., 2009; references in Retallack, 2009 and Breecker et al., in press). Furthermore, recent soil calibration studies of four Holocene carbonate-bearing soils indicate a total soil CO_2 (~500–2500 ppmv) during the period of likely carbonate precipitation (Breecker et al., 2009). These estimates indicate $S(z)$ contents that are half to up to an order of magnitude lower than used in previous paleo-atmospheric CO_2 reconstructions (see Section 5). These recent studies underscore the need for better constraints on total and respired soil CO_2 during carbonate formation including delineating any variability in this parameter by soil morphology and moisture regime, characteristics that can be confidently inferred from paleosols (Sheldon and Tabor, 2009).

3. MATERIALS AND METHODS

3.1. Two-component CO_2-mixing model for constraining soil CO_2

For soils characterized by two-component mixing of CO_2, the measured $\delta^{13}C$ of carbonate and contemporaneous SOM can be related to the concentration of total soil CO_2 by a two-component CO_2-mixing equation (Yapp and Poths, 1996):

$$[CO_2]_{soil}\,(\text{ppmv}) = \frac{(\delta^{13}C_{cc\text{-}a} - \delta^{13}C_{cc\text{-}r})}{\delta^{13}C_{cc\text{-}m} - \delta^{13}C_{cc\text{-}r})} \times [\text{atm } CO_2]\,(\text{ppmv}) \quad (2)$$

where the numerator is the difference in calculated $\delta^{13}C$ of carbonate that would form in isotopic equilibrium with either of the two end-members of CO_2 in a soil profile/horizon: (1) soil-respired CO_2 ($\delta^{13}C_{cc\text{-}r}$) and (2) the atmospheric component ($\delta^{13}C_{cc\text{-}a}$). The denominator is the difference in $\delta^{13}C$ of the measured carbonate ($\delta^{13}C_{cc\text{-}m}$) and $\delta^{13}C_{cc\text{-}r}$. Assuming a prescribed atmospheric CO_2 concentration and $\delta^{13}C$ value permits the equation to be solved for the total CO_2 content during calcite precipitation. Soil-respired CO_2, or the $S(z)$ parameter used in the paleosol-carbonate CO_2-barometer is the total soil CO_2 minus atmospheric CO_2.

This approach, however, requires that the carbonate formed in an aerated soil in which there is free exchange between the soil atmosphere and the overlying troposphere. Soils that are seasonally saturated by precipitation or a rising groundwater table may have periods of the year of limited gaseous diffusion between the two CO_2 reservoirs leading to a closed system in which soil CO_2 is derived solely from soil respiration (Sheldon and Tabor, 2009; Gulbranson et al., 2011a). Carbonate that formed during periods of closed system behavior would be inappropriate for this method of constraining total soil CO_2 (Tabor et al., in press). Similarly, soils characterized by three-component CO_2 mixing, given the added component of host rock, detrital or eolian carbonate (Rabenhorst et al., 1984; Amundson, 1989), are also inappropriate for this approach.

3.2. Dataset

Large datasets of calcite-bearing soils for which the $\delta^{13}C$ values of contemporaneous carbonate and SOM are known, the assumption of two-component soil CO_2 mixing is reasonable, and the climate regime is constrained, provide an opportunity to evaluate how total soil CO_2 varies between soil types and soil moisture regimes given their widespread geographic distribution and broad representation of soil conditions that dampen the effects of local site

and profile variability. Here, the measured $\delta^{13}C$ values of paired carbonates and SOM from a suite of 130 middle to late Holocene soils from the literature and unpublished data that represent six of the 12 soil orders and sub-humid to arid conditions of tropical, subtropical and temperate zones (Fig. 2) were applied to the two-component CO_2-mixing equation. The database (Appendix A) includes soils associated with C3 vegetation (20%), C4 vegetation (5%), and mixed C3–C4 flora (many of which are C3-dominated); carbonate–SOM pairs represent 233 horizons within these 130 different soils. Seasonal distribution of soil or air surface temperatures and precipitation, where not reported, was obtained from related published studies or from the NOAA National Climatic Data Center (http://www.ncdc.noaa.gov).

Many of the studies represented in Appendix A document down-profile increases or invariance in $\delta^{13}C_{carb}$ (e.g., Quade et al., 1989; Pendall and Amundson, 1990; Kelly et al., 1991; Wang et al., 1993; Amundson et al., 1994; Monger et al., 1998; Wang and Anderson, 1998; Buck and Monger, 1999; Miller, 2000; Zanchetta et al., 2000; Deutz et al., 2001, 2002; Landi, 2002; Salehi et al., 2004; Breecker et al., 2009; Laskar et al., 2010) compatible with carbonate formation in a soil characterized by two-component CO_2 mixing (Tabor et al., in press). Excluded from the dataset are gleyed profiles or those described as having extensive redoximorphic features, indicative of seasonal water-saturation, and/or with $\delta^{13}C_{carb}$ more negative than $-14‰$, which would require unlikely formation temperatures ($\geqslant 35$ °C) even for the most ^{12}C-enriched soil-respired CO_2 (derived from SOM of $-27‰$). For those studies (Landi et al., 2003; Mintz et al., 2011; Tabor et al., in press) documenting multiple generations of pedogenic carbonate or potential for calcite precipitation in a closed system, only the values of those calcites or profiles constrained petrographically, morphologically, and/or geochemically to have formed in a two-component system were used.

3.3. Constraining input parameters and uncertainty of estimates

3.3.1. $\delta^{13}C$ of soil-respired and total soil CO_2

The biologically respired component of CO_2 in soils is derived from two sources: (1) root respiration and (2) the microbial oxidation of SOM, with both varying seasonally and being highest during wet periods and the peak growth season. The $\delta^{13}C_{CO2}$ of root respiration can vary with shifts in the floral composition of overlying vegetation or with change in the degree of photosynthetic C isotope discrimination driven by changing environmental conditions (Farquhar et al., 1989; Arens et al., 2000). For soil carbonates, which likely form during the warm, drier period of the year (Breecker et al., 2009; Passey et al., 2010; Quade et al., 2011) when plant respiration is limited by decreasing soil moisture, it is likely that $\delta^{13}C_{carb}$ records a soil-respired CO_2 component dominated by microbially respired CO_2 (cf., Parker et al., 1983; Amundson et al., 1988). Moreover, given the fast turnover rates of labile ('fresh') organic matter, $\delta^{13}C_{SOM}$ may be the most appropriate proxy of respired CO_2 time-averaged over the period of pedogenic carbonate formation (Mora et al., 1996; although see below). In this study, the measured $\delta^{13}C$ value of SOM ($\pm 1\sigma$), reported for the same horizon from which the corresponding carbonate was sampled, was utilized as (1) a proxy of respired CO_2 and (2) to calculate the $\delta^{13}C$ values of a hypothetical calcite that would have precipitated from the soil-respired CO_2 end-member (see Section 3.3.3). For 23% of the soils, a profile average $\delta^{13}C_{SOM}$ was used given the lack of soil horizon-scale measurements (Appendix A).

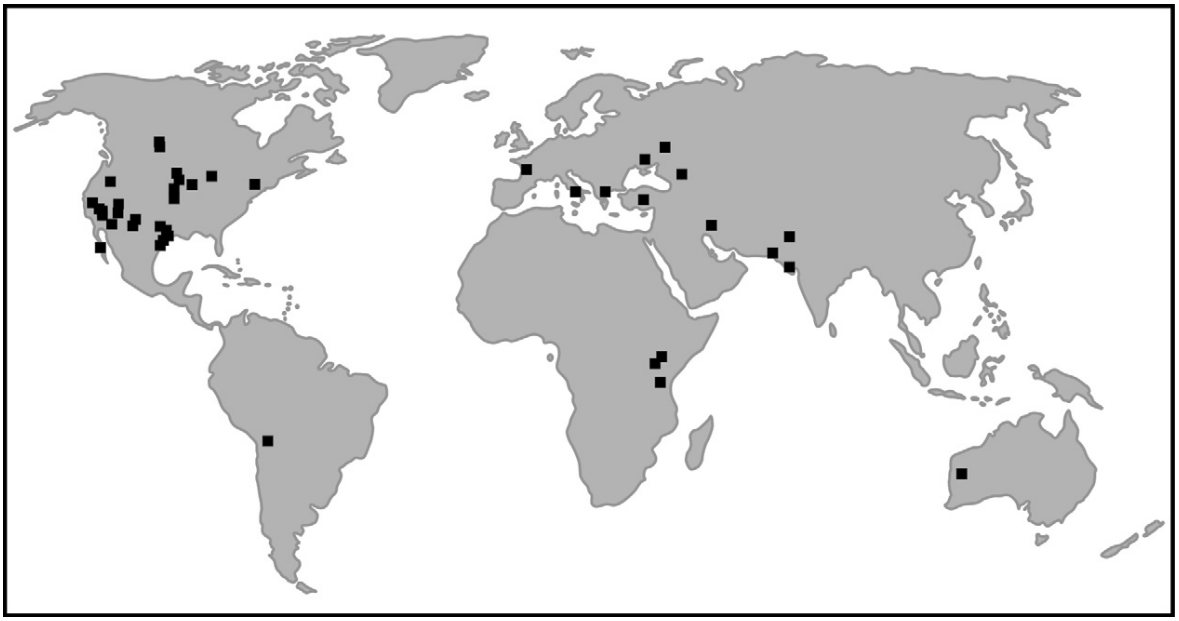

Fig. 2. World map (minus Antarctica) showing geographic distribution of soils used in this study.

One caveat to using the measured $\delta^{13}C_{SOM}$ as a proxy of $\delta^{13}C_{soil\text{-}respired\ CO2}$ is the potential of C isotope effects during decay of organic matter to impart a bias on total soil CO_2 estimates (cf. Bowen and Beerling, 2004). Selective use of organic compounds and C isotope discrimination during microbial decomposition of organic matter can lead to a <1 to several ‰ enrichment in the $\delta^{13}C$ of residual SOM (Nadelhoffer and Fry, 1988; Wedin et al., 1995). This C isotope effect contributes, in part, to the creation of down-profile increases in $\delta^{13}C_{SOM}$, which may not be reflected in $\delta^{13}C_{soil\ CO2}$ during calcite precipitation. Thus, the preferential decay of more labile organic matter may lead to a $\delta^{13}C_{soil\text{-}respired\ CO2}$ that is ^{12}C-enriched relative to the $\delta^{13}C$ of more refractory, and subsequently analyzed, SOM (Bowen and Beerling, 2004).

If such an offset between the $\delta^{13}C$ of soil CO_2, in which the sampled pedogenic carbonates formed, and that inferred from measured SOM exists in profiles/horizons used in this study, then the total soil CO_2 contents derived using the two-component CO_2-mixing equation would be overestimated. The degree of overestimation is dependent on the amount of $\delta^{13}C$ offset and the relative contribution of respired CO_2 to the total soil CO_2 pool, but could be on the order of 50% or greater (Fig. 3). Notably, studies of modern tropical and temperate soils, including field incubation studies, indicate minimal (≤0.5‰) offset between $\delta^{13}C_{soil\text{-}respired\ CO2}$ and $\delta^{13}C_{SOM}$ regardless of moisture regime (e.g., Santruckova et al., 2000; Stevenson et al., 2005; Rovira and Vallejo, 2008). Furthermore, this effect may be generally minimized given that soil microbes preferentially use ^{13}C-enriched compounds for biosynthesis that would counterbalance ^{13}C-discrimination during microbial respiration of CO_2 (Santruckova et al., 2000). The decay-related C isotope effect would be further dampened if calcite precipitation is thermodynamically favored in the warm, drier months when primary productivity, root respiration, and the addition of fresh labile organic matter to the soil is reduced relative to during the main growing season.

Of studies used in this compilation, the vast majority document a *decrease* in $\delta^{13}C_{SOM}$ values or invariance with depth; where nonlinear trends exist they have been attributed to independently inferred changes in the local floral composition (e.g., Kelly et al., 1991; Wang et al., 1996; Zanchetta et al., 2000; Deutz et al., 2001; Landi, 2002; Kovda et al., 2006; Miller et al., 2007; Laskar et al., 2010). Furthermore, most of these aforementioned studies document systematic parallel and consistently offset trends in $\delta^{13}C_{carb}$ and $\delta^{13}C_{SOM}$. Those that document a down-profile increase in $\delta^{13}C_{SOM}$, which is not attributable to an increase in the contribution of C4 vegetation to SOM, exhibit a shift of ≤1‰ (Wang and Anderson, 1998; Kovda et al., 2006), with one exception (~3‰; Salehi et al., 2004). It is thus concluded that the degree of overestimation of total soil CO_2 contents in this study due to decay-related C isotope effects is minimal, in particular for CO_2 estimates below 5000 ppmv (see Fig. 3 for further detail).

In an open system, the soil CO_2 reservoir is ^{13}C-enriched by minimally 4.4‰ relative to the soil-respired CO_2 flux ($\delta^{13}C_{cc\text{-}r}$) due to differences in the diffusion coefficients of $^{12}CO_2$ and $^{13}CO_2$ (Cerling et al., 1991), although effective

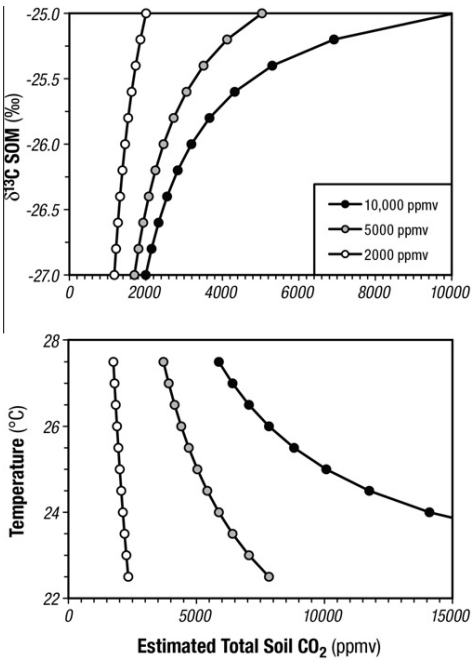

Fig. 3. Sensitivity of the two-component CO_2-mixing equation to variation in $\delta^{13}C_{SOM}$ and temperature of calcite precipitation. Top diagram: trend lines delineate the amount of overestimation of soil CO_2 with increasing offset (0‰ to −2‰) between measured $\delta^{13}C_{SOM}$ (−25‰) and actual $\delta^{13}C_{soil\text{-}respired\ CO2}$ present during calcite formation, assuming an initial soil CO_2 of 2, 5 or 10 K ppmv. For a 2‰ offset due to decay-related C isotope effects, soil CO_2 estimates would be overestimated by 40–80%. A 0.5–1‰ offset would reduce the degree of overestimation to <20–40% for those CO_2 estimates below 5000 ppmv. Lower diagram: trend lines delineate the amount of over- or under-estimation of soil CO_2 with changing temperature (up to ±3 °C) assuming initial conditions of soil CO_2 of 2, 5 or 10 K and 25 °C. The impact of temperature uncertainty on soil CO_2 estimates is minimal for low soil CO_2 and increases markedly with CO_2 contents of >5000 ppmv.

fractionation in natural soils may be lower (e.g., 4.24‰; Davidson; 1995). In this study, the reported $\delta^{13}C_{SOM}$ values were adjusted by +4.4‰ prior to calculating $\delta^{13}C_{cc\text{-}r}$. The CO_2 estimates, in the range of 1000–8000 ppmv, reported here would be lower or higher by <2 to ~25% for an effective fractionation 0.2‰ lower/higher than +4.4‰.

3.3.2. Atmospheric $\delta^{13}C$ and $[CO_2]$

An atmospheric CO_2 content of 300 ppmv, representative of mid-to-late Holocene to early industrial CO_2, was used in this study given that radiometric age constraints for many of the soils indicate they formed over the past few thousand years (e.g., Amundson, 1989; Pendall and Amundson, 1990; Kelly et al., 1991; Wang et al., 1996; Monger et al., 1998; Buck and Monger, 1999; Zanchetta et al., 2000; Deutz et al., 2001; Landi, 2002; Kovda et al., 2006; Laskar et al., 2010; Mintz et al., 2011). A preindustrial $\delta^{13}C$ value of −6.5‰ was utilized for atmospheric $\delta^{13}C$ (Francey et al., 1999). It should be noted that those soils in the dataset, which lack radiocarbon ages, could be older than mid-to-late Holocene and possibly be polygenetic if

they were actively forming over time spans exceeding the past few thousand years given the climate shifts of the last deglaciation.

3.3.3. Calculated end-member pedogenic calcite

The $\delta^{13}C$ value of pedogenic calcite that forms in a soil is dependent on the temperature of precipitation. For this study, the $\delta^{13}C$ values of hypothetical calcites that would precipitate from the soil-respired or atmospheric CO_2 end-members were calculated using a range of soil or air surface temperatures for each locality. A 'best estimate' of temperature was defined for each site using the mean value for the months during which time temperatures exceed, and precipitation is less than, the mean annual values (i.e., warm periods of decreasing to minimum precipitation; Appendix A). For example, for the Chihuahuan Desert of New Mexico, which is characterized by a late summer monsoonal climate, the period during which soil temperatures are high and precipitation is lowest (Serna-Perez et al., 2006) and minimum calcite solubility and apparent isotopic equilibrium between soil CO_2 and soil water is reached (Breecker et al., 2009), is the late spring-earliest summer. For other seasonal climates, the best estimate of temperature during the period of likely carbonate formation may be the mean for the late summer/early fall (late growing-season; cf. Retallack, 2009). When minimum calcite solubility occurs in seasonal soils is likely dictated by the temporal relationship between the seasonal distribution of rainfall, annual evapotranspiration, and temperature (cf. Gulbranson et al., 2011b).

The 'best estimate' of total soil CO_2 was calculated using the aforementioned temperature estimate for each location and the associated min/max range was defined using 1σ around the mean of measured $\delta^{13}C_{carbonate}$ and $\delta^{13}C_{SOM}$ values. Estimates of extreme maximum soil CO_2 were calculated using a minimum temperature (6–15 °C; Appendix A), constrained for each locality, excluding those months during which time the ground is frozen, covered with snow, and/or is likely to experience downward movement of snowmelt water. Estimates of extreme minimum soil CO_2 were made using the peak monthly temperature for a region regardless of precipitation level. For those few localities for which intra-annual soil or surface temperatures are not available, a temperature range of 10–25 °C was used. For extreme maximum (minimum) estimates, the most negative (positive) $\delta^{13}C_{carbonate}$ and the most positive (negative) $\delta^{13}C_{SOM}$ values, defined by 1σ around the mean of measured $\delta^{13}C$ values, were utilized.

Uncertainty in the temperature of carbonate formation translates to further uncertainty in total soil CO_2 estimates, with under-estimation of temperature leading to over-estimated CO_2 levels and vice versa (Fig. 3). This temperature-bias increases with magnitude of estimated soil CO_2 leading to a much smaller degree of uncertainty at the lower range of estimates (1000–2000 ppmv) than at the higher range (>5000 ppmv). The uncertainty in calcite precipitation temperature on estimated soil CO_2 values, however, is largely accounted for in the reported ranges of soil CO_2 estimates (Table 1) given the large temperature range (8–17 °C) used for each calculation (Appendix A).

4. RESULTS

4.1. Equilibrium vs. non-equilibrium carbonate–SOM pairs

For this approach to yield meaningful soil CO_2 estimates, the measured pedogenic carbonates and SOM must be contemporaneous. Temporal variations in the floral composition of associated vegetation coupled with translocation of organic matter through the soil profile could lead to present-day co-occurrence of carbonates and SOM that are not contemporaneous. Furthermore, if isotopic equilibrium fractionation is not maintained during carbonate precipitation then $\delta^{13}C_{carb}$ values do not record the soil atmosphere. Application of the $\delta^{13}C$ values of such carbonate–SOM pairs to the two-component CO_2-mixing equation would yield meaningless estimates of total soil CO_2.

In this study, $\delta^{13}C$ values of carbonates and SOM in corresponding horizons or profiles (Fig. 4) correlate positively ($r^2 = 0.48$) supporting that the majority of carbonate–SOM pairs are contemporaneous. In modern soils characterized by moderate to [high] respiration rates, calcite that forms in C isotopic equilibrium with the soil CO_2 will have a $\delta^{13}C$ between ~12‰ and 16‰ higher than contemporaneous SOM given that temperatures of carbonate formation typically range from well above freezing ($\geqslant 5$ °C) to $\sim 30 \pm 5$ °C, and assuming that SOM is the primary source of oxidized CO_2 to total soil CO_2 (Cerling, 1991). This range (specifically 12.2–15.8‰) in $\Delta^{13}C$ ($\delta^{13}C_{cc} - \delta^{13}C_{SOM}$) utilizes the $CO_{2(g)}$–calcite fractionation factor of Romanek et al. (1992) and is ~2‰ lower than previously proposed $\Delta^{13}C$ values of 14–16‰ (Cerling, 1991; Kelly et al., 1991; Cerling and Quade, 1993). The $\delta^{13}C$ values of carbonate–SOM pairs define two populations: (1) a subset ($n = 110$) that falls within the expected 'equilibrium' $\Delta^{13}C$ range, and (2) a subset ($n = 123$) that falls outside this range with $\Delta^{13}C$ values <12.2‰ (35 °C) or >15.8‰ (5 °C). All of the soils associated with C4 flora and 48% of those associated with purely C3 flora are included in the equilibrium population. Regression analysis of this population (herein referred to as 'equilibrium pairs') reveals a strong scaling relationship between their $\delta^{13}C_{carb}$ and $\delta^{13}C_{SOM}$ values ($r^2 = 0.87$) with an intercept of 14.1‰ suggesting an effective $\Delta^{13}C$ of ~14‰ (Fig. 4; cf. Wang and Anderson, 1998; Landi et al., 2003). A mean precipitation temperature of 20 °C ± 0.6 °C is inferred from this $\Delta^{13}C$ and falls within a few degrees of soil temperatures (16–18 °C) measured during the period of inferred isotopic equilibrium in the soil gas–water–calcite system in modern soils from central New Mexico (Breecker et al., 2009).

In contrast, the $\delta^{13}C$ values of carbonate–SOM pairs in the second population are not correlated ($r^2 = 0.14$) and define a broad range of $\Delta^{13}C$ (Fig. 4). The lack of apparent C isotopic equilibrium for these carbonate–SOM pairs (herein referred to as 'non-equilibrium pairs') could indicate that the measured carbonate and corresponding SOM are not contemporaneous. Sixty-one percent of the non-equilibrium pairs are from sites of mixed C3 and C4 flora; for several, temporal change in the C3:C4 vegetation ratio during the period of soil formation has been inferred (references listed in Appendix A). Translocation of organic matter

Table 1
Mean and range of measured soil parameters and estimated total soil CO_2 presented by soil order and vegetation.

Soil order (*n*)[a] Vegetation[b]	$\delta^{13}C_{cc}$ ±2 std. err. ‰	$\delta^{13}C_{SOM}$ ±2 std. err. ‰	Temp °C ± 2 std.[c] err. (min–max)	Total soil CO_2[d] $12.2 \leqslant \Delta^{13}C \leqslant 15.8$ (2 std. err. range) ppmv	Total soil CO_2[e] $12.1 \geqslant \Delta^{13}C \geqslant 15.9$ (2 std. err. range) ppmv	Min[f] total soil CO_2 ppmv	Max[g] total soil CO_2 ppmv
Mollisols (97)	−5.8 ± 0.5	−22.9 ± 0.7	19.3 ± 0.9 (6–35)	2266 (783–4180)	1093 (880–1449)	782 ± 50	2796 ± 742
C3 (29)	−8.4 ± 0.5	−25.1 ± 0.4	23.1 ± 1.2 (6–30)	3180 (1102–5352)	1166 (879–1420)	907 ± 223	2847 ± 1044
C4 (4)	−0.8 ± 0.9	−15.2 ± 1.4	25.3 ± 1.3 (10–27)	1830 (557–3632)	–	–	–
Alfisols: *C3* (16)	−7.8 ± 0.4	−25.0 ± 0.3	20.7 ± 0.7 (10–35)	1715 (1180–3280)	1248 (865–1649)	933 ± 76	3988 ± 2784
Aridisols: (45)							
Conifer woodland (4)	−7.3 ± 1.3	−22.2 ± 2.6	17.5 ± 2.2 (10–21)	3343 (858–5217)	nc	nc	4459 ± 1376
Desert shrubland (41)	−4.8 ± 0.8	−22.0 ± 1.1	25.2 ± 1.4 (10–43)	2038 (615–2126)	857 (619–998)	991 ± 269	2922 ± 1374
C3 (13)	−6.5 ± 1.6	−24.5 ± 0.4	22.8 ± 3.1 (10–32)	1878 (694–2527)	1043 (563–1523)	1372 ± 443	2071 ± 997
Vertisols: (48)							
Wooded grassland *(10)*	−7.5 ± 2.2	−20.8 ± 2.9	23.9 ± 1.8 (11–28)	2599 (967–9998)	nc	nc	3487 ± 2172
Wooded grassland *C3 (5)*	−10.1 ± 0.7	−25.2 ± 0.6	24.9 ± 1.5 (11–28)	2784 (979–9998)	nc	nc	–
Microhighs *(23)*	−4.8 ± 1.0	−20.1 ± 1.4	25.0 ± 0.4 (6–30)	1872 (934–2960)	590 (448–948)	1361 ± 752	3111 ± 1920
Microlows *(15)*	−6.8 ± 1.7	−23.5 ± 2.0	24.3 ± 0.7 (10–30)	15,276 (1202–26,477)	656 (515–787)	–	–
Microlows *C3 (4)*	−11.9 ± 0.3	−25.5 ± 0.1	22.0 ± 0.0 (10–25)	22,105 (7634–24,500)	nc	7141 ± 2220	nc
Andisols *C3* (10)	−11.3 ± 0.6	−26.2 ± 0.7	25.0 ± 0.2 (20–30)	6718 (2250–13,502)	1487 (1329–1560)	2355 ± 753	8059 ± 6410
Inceptisols (16)	−4.2 ± 0.8	−22.0 ± 0.9	27.2 ± 3.2 (15–43)	nc	635 (527–910)	501 ± 52	851 ± 161
C3 (5)	−2.4 ± 0.3	−22.9 ± 0.0	18.0 ± 0.0 (15–18)	nc	613 (578–648)	nc	655 ± 40

[a] Count includes number of soils per category. Actual number of soils used in total soil CO_2 mean and standard error values are sometimes fewer given that negative values were not included; see Section 4.2 and Appendix A for details.

[b] Vegetation refers to composition of overlying flora and/or inferred from $\delta^{13}C$ of soil organic matter (SOM). Unlabeled 'counts' indicate mixed C3 and C4 flora overlying the soil and/or inferred from SOM.

[c] Mean temperature (±2 std. err.) for months during which pedogenic carbonate precipitation is considered most likely; for each location as described in text; parenthetic temperature range spans lowest and highest monthly temperatures for locations during which time the ground is not frozen or snow covered and excludes those months of maximum precipitation. Soil temperatures used where reported; all other temperature estimates are surface air temperature as reported or obtained from http://www.climate-charts.com. See Appendix A for temperatures specific to each locality.

[d] Best estimate of total soil CO_2 for those soils for which $\Delta^{13}C_{cc\text{-}SOM}$ is within the anticipated range of isotopic equilibrium (12.2–15.8‰). Estimates based on paired measurements of $\delta^{13}C$ of pedogenic carbonate and SOM and mean temperature reported in footnote c; reported range defined by 2 × std. err. around estimates for (a) a likely lowest total soil CO_2 content calculated using highest $\delta^{13}C_{carb}$ and lowest $\delta^{13}C_{SOM}$, and (b) a likely highest total soil CO_2 content calculated using lowest $\delta^{13}C_{ped\ carb}$ and highest $\delta^{13}C_{SOM}$ and temperature in footnote c. Estimates >25,000 were not included in mean/range estimates (see Section 4.2).

[e] Best estimate of total soil CO_2 for those soils for which $\Delta^{13}C_{cc\text{-}SOM}$ falls outside the anticipated range of isotopic equilibrium (<12.2‰ and >15.8‰). Estimates calculated as in footnote d. Estimates >25,000 were not included in mean/range estimates (see Section 4.2).

[f] Extreme minimum estimate of total soil CO_2 for all soils calculated using maximum temperature at each locality and highest $\delta^{13}C_{carb}$ and lowest $\delta^{13}C_{SOM}$ values. A 'nc' indicates not calculated given no distinction made between peak and 'best' temperature estimates or a dominance of negative calculated values. Note, extreme minimum values above the range reported for 'best estimate of total soil CO_2: $12.2 \geqslant \Delta^{13}C \geqslant 15.8$' reflect that values include soils that fell within or outside of the anticipated range of isotopic equilibrium. Estimates >25,000 were not included.

[g] Extreme maximum estimate of total soil CO_2 for all soils calculated using minimum temperature at each locality during which time the ground is not frozen or snow covered and excluding those months of maximum precipitation, and lowest $\delta^{13}C_{carb}$ and highest $\delta^{13}C_{SOM}$ values. Note, maximum values below the range reported for 'best estimate of total soil CO_2: $12.2 \leqslant \Delta^{13}C \leqslant 15.8$' reflect that these values include soils within and outside of the anticipated range of isotopic equilibrium. Estimates >25,000 were not included in mean/range estimates.

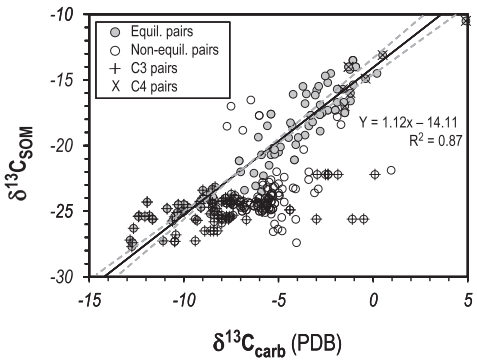

Fig. 4. Relationship between $\delta^{13}C$ of pedogenic carbonate and coexisting SOM. Paired $\delta^{13}C$ values for all equilibrium pairs (gray-filled circles) from individual horizons or soils define a significant positive correlation (r^2 of 0.87) with a slope of 1.124 and y-intercept of −14.1‰; gray dashed lines are confidence intervals. $\delta^{13}C$ values of non-equilibrium pairs are not correlated (r^2 of 0.14). The subset of non-equilibrium C3 soils ($n = 8$) with $\delta^{13}C_{carb} \geqslant -3‰$ are Inceptisols.

within profiles, in particular Vertisols (e.g., Miller, 2000; Miller et al., 2007), could have led to coexisting carbonate and SOM that are not contemporaneous. $\Delta^{13}C$ values of non-equilibrium pairs could alternatively record (1) soil-respired CO_2 at the time of carbonate precipitation dominated by root-respired CO_2 of different $\delta^{13}C$ value than that of the measured SOM or (2) changing $\delta^{13}C$ composition of bulk SOM due to the influx of fresh organic matter of a different C3:C4 ratio. The latter scenario is feasible given the order of magnitude difference in soil organic C turnover rates (10^1–10^2 yr), particularly in desert soils (Parker et al., 1983; Pendall et al., 1994) relative to rates of carbonate formation (10^2–10^3 yr) (Amundson et al., 1994; Wang et al., 1996).

However, for the large fraction of non-equilibrium pairs defined by $\Delta^{13}C$ values >15.8‰, it is also possible that they record either of two additional processes: (1) disequilibrium isotopic fractionation between CO_2 and soil water CO_3^{2-} leading to ^{13}C-enriched $\delta^{13}C_{carb}$ values (Rabenhorst et al., 1984) or (2) carbonate formation in a soil atmosphere of very low CO_2, as might be expected in low productivity dryland soils or soils with dynamic pore structures and conduits (e.g., Vertisols) (Brook et al., 1983; Breecker et al., in press; see Section 5.1). The non-equilibrium pairs (3%) with $\Delta^{13}C$ values <12‰ (i.e., open symbols above the regression line on Fig. 4) are all associated with mixed C3–C4 soils and thus can be accounted for by the aforementioned processes. For this group, formation in a soil atmosphere in which the soil-respired CO_2 component was ^{13}C-depleted relative to the measured SOM due to decay-related C isotope effects cannot be discounted. This group could alternatively record ^{13}C-depletion of total soil CO_2 due to decreased diffusivity between $^{13}CO_2$ and $^{12}CO_2$ driven by closed-system soil dynamics in saturated soils (Rovira and Vallejo, 2008; Tabor et al., in press). Importantly, this effect should be minimized in this study as soils observed or inferred to have been seasonally water-saturated for extended periods of time were excluded.

Applying non-equilibrium carbonate–SOM pairs, which record a change in local vegetation, disequilibrium isotopic fractionation, or decay related C isotope effects to the two-component CO_2-mixing model would lead to total soil CO_2 estimates that lack environmental significance. Therefore, in Section 4.2, estimates of total soil CO_2 made using equilibrium and non-equilibrium pairs are presented separately. CO_2 estimates from C3 or C4 soils are further considered separately given that the effect of changing flora on the $\delta^{13}C$ values of soil-respired CO_2 and SOM are expected to be minimal.

Negative values were obtained for 31% of the total soil CO_2 calculations and result from calculated $\delta^{13}C$ values of hypothetical calcites, which would have formed in a purely soil-respired CO_2 atmosphere ($\delta^{13}C_{cc\text{-}r}$), that are less negative than their corresponding measured $\delta^{13}C_{carb}$. This can result from the effects of the aforementioned processes and from the uncertainty in precipitation temperature. When the offset between hypothetical and measured carbonate $\delta^{13}C$ is small (e.g., ≪1‰, within the uncertainty of precipitation temperature) it is likely that negative soil CO_2 estimates are indicative of soils with very high CO_2 contents. This reflects that $\delta^{13}C_{cc\text{-}meas} - \delta^{13}C_{cc\text{-}r}$ asymptotically approaches zero at soil CO_2 contents in the 10^5-ppmv range. High estimates of soil CO_2 potentially recorded by some of the negative values in this study are therefore not represented in the soil order-specific estimates reported below. Soil CO_2 concentrations in the following sections are reported as two significant figures to reflect the uncertainty in measured C isotopic compositions and surface or soil temperatures and the propagation of these errors in the calculations. Actual calculated values are reported in Table 1 and Appendix A.

4.2. Soil order-specific results

4.2.1. Mollisols

Mollisols are grassland ecosystem soils that are characterized by an organic-rich surface horizon and a subsurface horizon(s) that shows evidence of clay illuviation (enrichment), commonly separated by a leached (albic) horizon (Soil Survey Staff, 2010). Ninety-seven carbonate–SOM pairs in this study represent individual horizons within 61 profiles of grassland Mollisols (Appendix A). Of these sets, 29 are associated with C3 vegetation of which 38% are equilibrium and 62% are non-equilibrium pairs. Four sets are associated with C4 vegetation and are equilibrium pairs. The remaining carbonate–SOM pairs, associated with mixed C3–C4 vegetation, consist of 33% equilibrium and 67% non-equilibrium pairs.

For equilibrium pairs, the best estimate (and range) of total soil CO_2 for Mollisols is 2300 ppmv (780–4200 ppmv), whereas for C3 and C4 equilibrium pairs specifically, it is 3200 ppmv (1100–5000 ppmv) and 1800 ppmv (560–3600 ppmv), respectively (Table 1). Non-equilibrium pairs yield an overall lower mean estimate of 1100 ppmv (880–1500 ppmv), with a best estimate of 1200 ppmv (880–1400) for C3 soils. Extreme minimum and maximum CO_2 estimates for all pairs are 780 ± 50 ppmv and 2800 ± 740 ppmv. Negative values were obtained for 5% of the best (range) soil

CO_2 estimates and 13% of the extreme maximum and minimum estimates. The reported ranges do not include two high values (53,700 and 57,900 ppmv) for C3 pairs and a value of 26,200 ppmv for a mixed C3–C4 pair.

4.2.2. Alfisols

Alfisols are moderately leached soils with a subsurface horizon(s) in which illuvial clays and potentially carbonates accumulate (Soil Survey Staff, 2010). Seventeen carbonate–SOM pairs represent individual horizons within eight Alfisol profiles (Appendix A). Sixteen are associated with C3 vegetation, of which 31% are equilibrium and 69% are non-equilibrium pairs. One non-equilibrium pair is associated with mixed C3–C4 vegetation. For equilibrium pairs, the best estimate (and range) of total soil CO_2 is 1700 ppmv (1200–3300 ppmv), whereas for non-equilibrium pairs it is 1300 ppmv (860–1700 ppmv) (Table 1). Extreme minimum and maximum CO_2 estimates, calculated using all pairs, are 930 ± 80 ppmv and 4000 ± 2800 ppmv. Negative values were obtained for 12% of the extreme maximum CO_2 estimates.

4.2.3. Aridisols

Aridisols form in regions characterized by a net soil-moisture deficit and exhibit limited leaching and at least some development of subsurface horizons in which $CaCO_3$ and other salts and clays accumulate (Soil Survey Staff, 2010). Forty-five of the carbonate–SOM pairs represent horizons within four conifer woodland and 41 desert shrubland Aridisol profiles (Appendix A). The conifer woodland pairs are all associated with mixed C3–C4 vegetation and are equilibrium sets. Thirteen of the desert shrubland pairs are associated with C3 vegetation, of which 46% are equilibrium and 54% are non-equilibrium sets. One equilibrium pair from a desert shrubland Aridisol is associated with C4 vegetation. The remaining sets ($n = 27$) are associated with mixed C3–C4 vegetation of which 59% are equilibrium and 41% are non-equilibrium pairs.

The conifer woodland equilibrium pairs yield a best estimate (range) of total soil CO_2 of 3300 ppmv (860–5200 ppmv) and an extreme maximum estimate of 4500 ± 1400 ppmv (Table 1). No negative values were obtained. For all desert shrubland equilibrium pairs, the best estimate (range) of total soil CO_2 is 2000 ppmv (610–2000 ppmv), whereas for C3 equilibrium pairs it is 1900 ppmv (690–2500 ppmv). Non-equilibrium pairs yield CO_2 estimates of 860 ppmv (620–1000 ppmv), with a slightly higher best estimate (1000 ppmv) and range (560–1500 ppmv) for C3 soils. Extreme minimum and maximum mean estimates for all desert shrubland Aridisols are 990 ± 270 ppmv and 2900 ± 1400 ppmv with overlapping values calculated for C3 pairs (Table 1).

Negative values were obtained solely for desert shrubland Aridisols, and include all values for the one equilibrium C4 pair, 8% of the best (range) estimates for mixed C3–C4 equilibrium pairs, and 24% of the extreme maximum estimates of soil CO_2 calculated using all pairs. The reported ranges do not include an anomalous high value (230,500 ppmv) for a C3 equilibrium pair and two high values (49,300 and 55,500 ppmv) for mixed vegetation pairs.

4.2.4. Vertisols

Vertisols are clay-rich soils that exhibit a subsurface horizon(s) with slickensides and/or wedge-shaped peds and subvertical cracks, which develop in response to seasonal changes in moisture content (Soil Survey Staff, 2010). Forty-eight of the carbonate–SOM pairs represent 17 wooded grassland Vertisol profiles (Appendix A). Of these, 11 pairs are associated with C3 vegetation, two with C4 vegetation, and the remaining with mixed C3–C4 flora. A large subset (76%) of these Vertisol pairs were sampled specifically within microhighs, microslopes or microlows and are discussed separately from carbonate–SOM pairs not differentiated by profile position. For the latter ($n = 15$), the C4 pairs are equilibrium, whereas 29% of the C3 ($n = 5$) and all of the mixed C3–C4 sets (3) are non-equilibrium pairs.

The wooded grassland equilibrium pairs define a best estimate (range) of total soil CO_2 of 2600 ppmv (980–10,000 ppmv), whereas the best estimate for C3 equilibrium pairs is 2800 ppmv (Table 1). No estimates of total soil CO_2 were obtained for the equilibrium C4 pairs or non-equilibrium C3 or mixed flora pairs as they yielded predominantly negative numbers. An extreme maximum estimate of 3500 ± 2200 ppmv was calculated on the basis of 65% of the wooded grassland carbonate–SOM pairs; the remaining yielded negative values.

For carbonate–SOM pairs ($n = 23$) that were sampled from the microhigh regions of five Vertisol profiles, two are associated with C3 vegetation and are equilibrium pairs and twenty-one are associated with mixed C3:C4 vegetation. Of the mixed vegetation set, 81% are equilibrium pairs. The microhigh equilibrium pairs define a best estimate (range) of total soil CO_2 of 1900 ppmv (930–3000 ppmv); no estimates were obtained specifically for the C3 pairs as 83% of calculated values were negative (Table 1). Non-equilibrium pairs from microhighs define a much lower best estimate (590 ppmv) and range (450–950 ppmv) of total soil CO_2. Extreme minimum and maximum CO_2 estimates, calculated using all pairs, are 1400 ± 750 ppmv and 3100 ± 1900 ppmv. In addition, 31% of the best (range) estimates for equilibrium C3–C4 pairs and 33% of the extreme minimum and maximum estimates were negative. The reported microhigh ranges do not include one anomalous value (26,200 ppmv).

For carbonate–SOM pairs ($n = 15$) that were sampled from the microlow and microslope regions of three Vertisol profiles (Appendix A), four are associated with C3 vegetation and are equilibrium pairs. The other 11 sets are associated with mixed C3–C4 vegetation of which 36% are equilibrium pairs. The microlow equilibrium pairs define a best estimate (range) of total soil CO_2 of 15,300 ppmv (1200–26,500 ppmv) with the subset of C3 equilibrium pairs defining a higher best estimate of 22,100 ppmv (range of 7600–24,500 ppmv). Microlow non-equilibrium pairs yield a much lower mean estimate (660 ppmv) and range (520–790 ppmv) of total soil CO_2. Extreme minimum and maximum estimates are not reported as 82% were negative values. Negative values were also obtained for 50% of the best (range) estimates based on C3 equilibrium pairs and 67% of the C3–C4 equilibrium pairs.

4.2.5. Andisols

Andisols are high water-holding capacity soils that develop uniquely in volcanic deposits and are thus the least extensive soil order (<1% of the ice-free land area). Ten of the carbonate–SOM pairs represent horizons within five Andisol profiles (Appendix A). All sets are associated with C3 vegetation and 70% are equilibrium pairs. For equilibrium pairs, the best estimate (range) of total soil CO_2 for Andisols is 6700 ppmv (2300–13,500 ppmv), whereas for non-equilibrium pairs it is 1500 ppmv (1300–1600 ppmv) (Table 1). Extreme minimum and maximum soil CO_2 estimates, calculated using all pairs, are 2400 ± 750 ppmv and 8100 ± 6400 ppmv. Negative values were obtained for 14% of the best (range) estimates and 20% of the extreme minimum and maximum CO_2 estimates. The reported ranges do not include an anomalous value of 28,800 ppmv.

4.2.6. Inceptisols

Inceptisols, along with Entisols, are immature soils that exhibit weak horizon development. Sixteen of the carbonate–SOM pairs represent eight Inceptisols (Appendix A). Of these sets, five are associated with C3 vegetation and are non-equilibrium pairs. Eleven sets are associated with mixed C3–C4 vegetation, and are dominantly (91%) non-equilibrium pairs. The best estimate (range) of total soil CO_2 based on equilibrium pairs is not reported given limited data. Non-equilibrium pairs yield a best estimate of total soil CO_2 of 640 ppmv (530–910 ppmv), which overlaps with that calculated for the subset of C3 soils (610 ppmv; range of 580–650 ppmv). Overall extreme minimum and maximum CO_2 estimates are 500 ± 50 ppmv and 850 ± 150 ppmv. Negative values were obtained for 10% of the best (range) estimates and for 17% of the extreme maximum CO_2 estimates. The reported ranges do not include an anomalous minimum value 7300 ppmv.

5. DISCUSSION

The soil order-specific CO_2 estimates obtained using equilibrium $\delta^{13}C_{cc} - \delta^{13}C_{SOM}$ pairs from C3 or C4 profiles are the most likely to characterize the soil atmosphere during periods of calcite precipitation for the reasons discussed in Section 4.1. Overall, the total soil CO_2 estimates (Table 1), made using equilibrium C3 or C4 pairs, fall within a range of ~600–6000 ppmv (with the exception of some Vertisols and Andisols), similar in span to that of measured soil CO_2 in modern carbonate-bearing soils (e.g., Soloman and Cerling, 1987; Amundson et al., 1988, 1994; Quade et al., 1989; Amundson and Davidson, 1990; Breecker et al., 2009; references within Breecker et al., in press). Uncertainty in temperature of calcite precipitation beyond that captured by the utilized temperature range or in the diffusion coefficients of $^{12}CO_2$ and $^{13}CO_2$, and the potential for undetected decay-related C isotope effects – all anticipated to be minimal as previously discussed (Section 3.3) – would bias the reported ranges toward *overestimated* total soil CO_2 concentrations.

The soil order-specific estimates further define a range of total soil CO_2 (Table 1) and soil-respired CO_2 ($S(z)$) (Fig. 5) for each soil order. The following discussion proposes best estimates and ranges of $S(z)$ considered most appropriate for application to the paleosol-carbonate CO_2-barometer. For grassland Mollisols and their paleosol analogs inferred throughout the Cenozoic and possibly late Cretaceous record (Prasad et al., 2005), a best estimate of $S(z)$ is 2500 ppmv with a range of ~600 ppmv to 4000 ppmv. Paleosol analogs of Alfisols, Aridisols, Vertisols, Inceptisols, and Entisols are common throughout the geologic record of the past 440 million years. For carbonate-bearing Aridisols and their paleosol equivalents (Calcisols), which are defined by a calcic subsurface horizon(s) that is the most prominent pedogenic feature (Mack et al., 1993), a best estimate of $S(z)$ is 1500–2000 ppmv. A similar best estimate is defined for Alfisols and their paleosol analogs (Argillisols), for which the most prominent feature is an argillic horizon that indicates clay enrichment (illuviation). The overall range for Aridisols (Calcisols) and Alfisols (Argillisols) of near atmospheric to ~5000 ppmv can be further constrained given that field-based studies of modern soils document an increase in soil pCO_2 with soil moisture, vegetation density, and/or elevation (e.g., Amundson et al., 1988; Quade et al., 1989; Stevenson et al., 2005). The low $S(z)$ range delineated by desert shrubland soils (<500–2500 ppmv) may be most appropriate for paleosols that formed in regions of net soil-moisture deficit, whereas a higher $S(z)$ range of 2000–5000 ppmv may better represent paleosols for which increased paleo-soil moisture, paleo-vegetation density, and/or paleo-elevation can be inferred. The near atmospheric levels (400 ppmv ± 200 ppmv) of inferred $S(z)$ in well-drained Inceptisols highlight the extremely low soil productivity during carbonate formation in immature soils and their paleosol analogs (Protosols).

Vertisols and paleo-Vertisols present a unique case in that estimates of total soil CO_2, and in turn $S(z)$), span a range from <1000 to >25,000 ppmv (Table 1; Fig. 5), which in large part reflects the disparity in soil CO_2 estimates between structural components. The disproportionate percentage of negative values for Vertisols (Appendix A) most likely reflects the unique hydrodynamic conditions of these profiles that results from the shrinking and swelling of clay-rich matrices in response to strongly seasonal precipitation (Soil Survey Staff, 2010). Limited data from field monitoring studies of Vertisols corroborate this finding in documenting overall lower soil CO_2 in microhighs than microlows and a greater than 2-orders of magnitude range (1000s to ~200,000 ppmv), with overall higher values in Vertisols during wetter than drier periods (Breecker et al., in press and references within).

Vertisols can become periodically water-logged during seasonal surface flooding or with a rising groundwater table leading to limited gaseous diffusion between the soil atmosphere and free-air. If $[Ca^{2+}]$ in soil pore-waters becomes sufficiently high in response to hydrolosis and/or calcite dissolution, carbonate will precipitate in a closed C system (cf. Rovira and Vallejo, 2008). For those Vertisols for which the difference between the $\delta^{13}C$ values of measured and hypothetical calcite, formed from 100% soil-respired, is $\ll 1‰$, it is likely that the negative soil CO_2 estimates indicate calcite precipitation under very high soil CO_2 contents, characteristic of a high soil-moisture, closed system. This

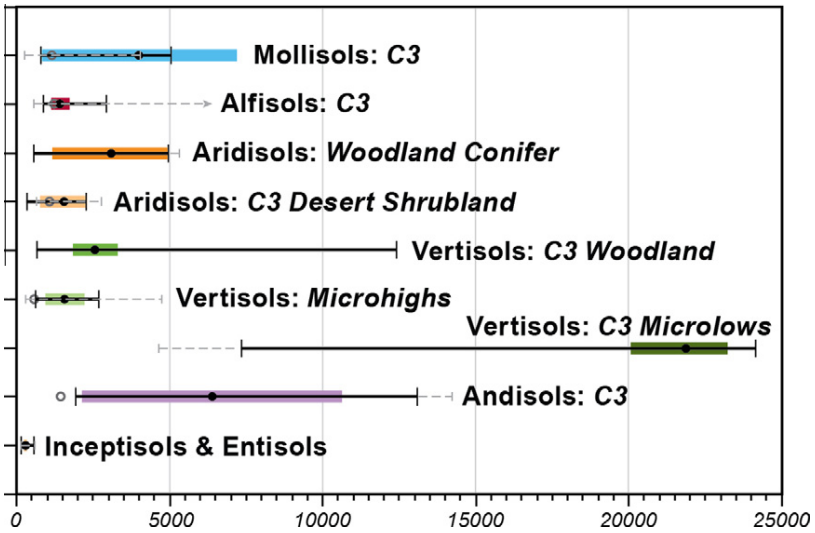

Fig. 5. Estimated ranges of $S(z)$ during carbonate precipitation in modern calcite-bearing soils associated with C3, C4, or mixed flora, presented by taxonomic soil order. Colored bars indicate the range defined by the mean (±2 std. err.) of all 'equilibrium pairs' within a taxonomic set or the C3 soil subset. Mean values shown by filled circles for 'equilibrium pairs' and open circles for 'non-equilibrium pairs'. Solid horizontal lines extending from the colored bars delineate the ±2 std. err. around the mean of all minimum and maximum estimates calculated for each equilibrium pair within a soil order. Dashed lines define the extreme minimum and maximum range calculated using minimum and maximum temperatures (see footnotes of Table 1 for more detail). (For interpretation of the references to color in this figure legend, the reader is referred to the web version of this article.)

interpretation is supported by the very high CO_2 estimates (>25,000–56,000 ppmv) obtained for several carbonate–SOM pairs from Vertisol microlows and microslopes. The negative estimates, derived from Vertisol carbonate–SOM pairs that include all those with a $\Delta^{13}C < 12‰$, could also record decreased diffusivity between $^{13}CO_2$ and $^{12}CO_2$ under closed system dynamics that would be recorded as anomalously low $\delta^{13}C_{carb}$ values (Tabor et al., in press). Notably, estimates of soil CO_2 derived from carbonates that precipitated in a closed system do not record the mixing of two components of CO_2 and are thus inappropriate for application to the paleosol-carbonate CO_2-barometer.

The significantly lower inferred levels of $S(z)$ for Vertisol microhighs and overall wooded grassland Vertisols (Fig. 5) suggests that carbonate precipitation in the well-drained portions of Vertisols occurs primarily during free exchange between the soil and troposphere CO_2 reservoirs. Seasonal fluctuations in the hydrochemistry of Vertisols could lead to shifts between closed- and open-system behavior promoting carbonate dissolution–precipitation cycles (Rovira and Vallejo, 2008; Mintz et al., 2011). Field calibration and modeling studies suggest that calcite formation in such soils may be thermodynamically favored during rapid degassing and decrease in soil pCO_2 with seasonal turnover from closed to open system dynamics driven by decreased soil moisture, development of crack conduits, and restructuring of the pore networks (Breecker et al., in press; cf. Rovira and Vallejo, 2008). The near atmospheric levels of $S(z)$ suggested by non-equilibrium pairs with a $\Delta^{13}C > 16‰$, could indicate the extremely low levels of total soil CO_2 during such periods (Mintz et al., 2011) or could potentially record disequilibrium isotopic fractionation during periods of rapid degassing. In the context of these processes and the complex hydrochemical nature of Vertisols, a best estimate $S(z)$ of 2000 ppmv ± 1000 ppmv is most appropriate for paleo-Vertisols for which evidence of extended water saturation (gleying and redoximorphic features) is minimal. A $S(z)$ range extending to ~5000 or possibly 10,000 ppmv (or higher) is possible for profiles for which a net negative soil moisture deficit is inferred. Ultimately, better constraints on the appropriate range of $S(z)$ during calcite precipitation in Vertisols will require field monitoring studies of the complex hydrochemical dynamics of these soils such as those being carried out by Breecker and colleagues (in press).

5.1. Evaluation of the accuracy and precision of soil CO_2 estimates

Studies of modern soils with well-constrained vegetation and which include seasonal measurements in total soil CO_2 content and $\delta^{13}C$, soil and/or surface temperature and $\delta^{13}C$ of soil carbonates provide an opportunity to evaluate how well the method of applying $\delta^{13}C_{carb}$ and $\delta^{13}C_{SOM}$ pairs to the two-component CO_2-mixing model approximates actual soil CO_2 concentrations. Monitored soils ($n = 8$) from a range of elevations (840–1900 m) in the southern Great Basin and central New Mexico (Amundson et al., 1988; Amundson, 1989; Quade et al., 1989; Breecker et al., 2009) were used to compare field soil CO_2 measurements to CO_2 estimated by the approach described in this study (Table 2). In order to best replicate the mixing model method, $\delta^{13}C_{SOM}$ was inferred from measured $\delta^{13}C_{veg}$, where reported, or estimated based on surveyed abundance of C3 ($\delta^{13}C$ of −27‰), C4 (−12‰), and CAM (−15‰) plants at each site. This approach additionally avoids the

Table 2
Comparison of measured vs. estimated total soil CO_2 for low elevation Holocene dryland soils.

Locality and soil order (study)	Locality conditions[a]	Total soil CO_2 Measured (ppmv)	Total soil CO_2 best estimated range (ppmv)	Maximum est. range (ppmv)
Eastern Mojave, southern Great Basin, Spring Mountains, NV, USA: desert shrubland Aridisol (Amundson et al., 1988; Amundson, 1989)	Elevation: 1400 m Temp: 23.5 °C (18–29 °C) $\delta^{13}C_{carb}$: −3.8‰ (−4.8‰ to −0.5‰) $\delta^{13}C_{CO2}$: −19.0‰ to −8.5‰	Mean (25–75 cm): 971 April: 691 ± 493–1974 ± 1450 September: 395–987 ± 99	Best (range): 832 (387–1665)[b]	382–2786
Southern Great Basin, Spring & Grapevine Mtns., NV, USA: desert shrubland Aridisols (Quade et al., 1989)	Temp: 19.5 °C MAT (10–29 °C) $\delta^{13}C_{carb}$: −2.8‰ (−5.4‰ to −1.1‰) $\delta^{13}C_{soil\text{-}respired\ CO2}$: −25.6‰ to −14.0‰			
	Spring Mountains: 840 m	April: 1650[c] September: 600	Best (range): 459 (417–977)[d]	406–1933
	Grapevine Mountains: 900 m	April: 1025 September: 800	Best (range): 595 (452–1032)	437–1534
	Grapevine Mountains: 1160 m	April: 1100 September: 850	Best (range): 571 (469–845)	406–1933
	Spring Mountains: 1550 m	April: 1725 September: 990	Best (range): 765 (558–1605)	542–4285
Sevilleta National Wildlife Refuge, central NM, USA: Entisols & Inceptisols (Breecker et al., 2009)	Temp: 16–18 °C (equil $CaCO_3$ precip.) $\delta^{13}C_{carb}$: −2.0‰ (−4.0‰ to 1‰) $\delta^{13}C_{soil\text{-}respired\ CO2}$: −26.5‰ to −19.5‰			
	Chihuahuan Desert shrubland: 1450 m	May: 1000[e] (900–1500) (756–1632)[f]	Best (range): 511 (410–759)[g]	399–921
	Great Basin shrubland: 1475 m	May: 700 (700–1500)	Best (range): 463 (337–957)	334–1335
	Pinon Juniper woodland: 1900 m	May: 2500 (1900–4000)	Best (range): 640 (425–2076)	411–8461

[a] Conditions reported in cited publication(s). Additional temperature information from NOAA National Climatic Data Center. $\delta^{13}C_{soil\text{-}respired\ CO2}$ for months of lower than average precipitation at each site see "Veracity Test: Holocene Soils" in Appendix A. Range in $\delta^{13}C_{carb}$ for Breecker et al. (2009) from depths of 42–70 cm at all sites (three profiles).

[b] Calculated using the following: (1) Best estimate of $\delta^{13}C_{soil\text{-}respired\ CO2}$ based on $\delta^{13}C_{SOM}$ inferred using the surveyed plant cover in September at the study site of 37.9% C4, 59.1% C3, and 3% CAM vegetation (Amundson et al., 1988) and $\delta^{13}C$ values of −12‰, −27‰, and −15‰, respectively. Range defined using a $\delta^{13}C_{veg}$ of −25‰ proposed by Amundson et al. (1988) and +2‰ over the best estimate to account for decay-related C isotope effects or seasonal variation in floral or C isotopic composition of plant cover at the site. Notably, these estimated $\delta^{13}C_{soil\text{-}respired\ CO2}$ values differ by <0.5‰ from the range in $\delta^{13}C_{soil\text{-}respired\ CO2}$ reported by Quade and others (1989) for ~1400 m in the Spring Mountains and inferred using [soil CO_2] and $\delta^{13}C_{soil\ CO2}$ measured in April–May and September at 50 cm depth across an elevation transect of soil profiles in the Spring Mountains. (2) Avg. ±1σ of measured $\delta^{13}C_{carb}$ and MAT with temperature range from NOAA site for period of precipitation < MAP. See "Veracity Test: Holocene Soils" in Appendix A for site-specific values. (3) Extreme estimated range in soil CO_2 calculated as in Table 1.

[c] Measured soil CO_2 at 50 cm ± 10 cm (Quade et al., 1989).

[d] Calculated using the following: (1) Best estimate (±2‰) of $\delta^{13}C_{soil\text{-}respired\ CO2}$ based on $\delta^{13}C_{SOM}$ inferred from the surveyed plant cover at the study sites (Quade et al., 1989) and $\delta^{13}C_{veg}$ as in 'a'. (2) For Spring Mountain site #1 (840 m) a measured $\delta^{13}C_{veg}$ (−24.9‰) was used for the best and minimum (with an additional −2‰) estimate with a calculated high value of $\delta^{13}C_{soil\text{-}respired\ CO2}$ (−14‰) based on the possibility of a contribution of up to 40–50% by C_4 grasses and/or shrubs during the spring season at this site. (3) Average ± 1σ of measured $\delta^{13}C_{carb}$ and MAT with temperature range from NOAA site for period of precipitation < MAP. (4) Extreme estimated range in soil CO_2 calculated as in Table 1.

[e] Measured total soil CO_2 in May 2008 at 67 cm (Chihuahuan Desert shrubland), 62 cm (Great Basin shrubland), and 59 cm (Pinon Juniper woodland) depths in profiles; range in soil CO_2 over months of low precipitation and soil solution [Ca^{2+}] at each site, proposed as the period of likely carbonate precipitation (Breecker et al., 2009).

[f] Range of total soil CO_2 estimates for a series of Chihuahuan soils from Serna-Perez et al. (2006). Estimates calculated by applying to a Fickian one-dimensional diffusion equation (Cerling, 1984) the range of soil respiration flux (mg m^{-2} h^{-1}) during the period April through July, 2003 measured using NaOH traps at 50 cm soil depth at multiple sites on the Lower La Mesa geomorphic surface (800 ka ± 100 ky), Jornada Basin Long Term Ecological Research site, southern New Mexico, USA. Calculations used an atmospheric [CO_2] of 380 ppmv, a diffusion coefficient for gas through the soil of 0.0001, a 50 cm soil depth, and a scaling depth of 20 cm.

[g] Calculated using the following: (1) Best estimate (range of ±2‰) of $\delta^{13}C_{soil\text{-}respired\ CO2}$ based on inferred plant cover at the study sites (Breecker et al., 2009). A $\delta^{13}C_{veg}$ of −25‰ was used for the C3 Chuhuahuan Desert site; a 1‰ less negative $\delta^{13}C_{veg}$ was used for the predominantly C3 Great Basin site, and a conservative range of $\delta^{13}C_{veg}$ of −25‰ to −19‰ was used for the mixed C3–C4 Pinon-Juniper site

to reflect a measured $\delta^{13}C_{SOM}$ of −19‰ at the Grassland site (C4-rich end-member), interpreted to likely record an earlier component of C3 shrubs in the region (Breecker et al., 2009). Note, $\delta^{13}C_{soil\text{-}respired\ CO2}$ inferred from the measured $\delta^{13}C_{soil\ CO2}$ at each site using the method described in Davidson (1995) is 3–6‰ more negative than used here. (2) Average ± 1σ of measured $\delta^{13}C_{carb}$ from depths of 42–70 cm at each site and measured soil temperatures (between 59 and 67 cm depth) during periods of lowest rainfall and low soil solution [Ca^{2+}]. (3) Extreme estimated range in soil CO_2 calculated as in Table 1.

dependence of reported values of $\delta^{13}C_{soil\text{-}respired\ CO2}$ on measured soil CO_2 contents as calculated using the methods described in Davidson (1995) or Quade et al. (1989). All of the soils yield non-equilibrium $\Delta^{13}C$ ($\delta^{13}C_{carb} - \delta^{13}C_{SOM}$) values; further details regarding the calculations are presented in Table 2.

Comparison of the two sets of total soil CO_2 documents generally overlapping ranges but also indicates that for all sites, except the eastern Mojave soils, the estimated values are lower by 10–50% than the corresponding measured soil CO_2 (Table 2). The difference between the two sets of values is greatest for the minimum estimates and overall highest for the Entisols and Inceptisols of central New Mexico. In contrast, maximum estimated values of soil CO_2, which assume carbonate formation during colder temperatures, exceed the highest measured CO_2 contents by 15% to two-fold, a finding in accordance with previous studies that suggest carbonates form during the hot months of low precipitation. For two New Mexico *immature* soils, they underestimate the maximum measured CO_2 content by 11–40%. Notably, a strong correlation between measured maximum soil CO_2 and both estimated maximum ($r^2 = 0.86$) and extreme maximum CO_2 ($r^2 = 0.75$) indicates that the estimated values capture the *relative* differences in total soil CO_2 between the studied sites, including the observed trend of increasing soil CO_2 with elevation. These findings are maintained when the $\delta^{13}C_{soil\text{-}respired\ CO2}$ values reported in each study are substituted for $\delta^{13}C_{SOM}$ with estimated CO_2 contents between the two sets differing by 1% to ⩽30% (Appendix A). This comparison of measured and estimated soil CO_2 illustrates the potential of the mixing model approach for constraining paleosol $S(z)$ while further delineating the level of associated uncertainty (10–50%). The results also highlight the potential for near atmospheric levels of soil CO_2 in immature soils.

This comparison further indicates that the aforementioned proposed $S(z)$ ranges for those paleosols that can be inferred to have formed under conditions of low vegetation density and net soil-moisture deficit (Calcisols, some Argillisols and Vertisols) are reasonable for soil-respired CO_2 during calcite formation. For this subset of 'dryland' paleosols, the proposed $S(z)$ ranges overlap with but expand the 2500 ppmv $S(z)$ value recently suggested by Breecker et al. (2009, 2010) as being widely applicable for all carbonate-bearing paleosols. This study's results suggest a higher range of $S(z)$ values for paleosols that formed under higher soil moisture conditions. Morevoer, for application to paleosols, it is important to consider that all of the estimated soil CO_2 ranges would scale upwards with increased atmospheric pCO_2, with the scaling factor dependent on the ratio of paleo-CO_2/present-day CO_2. Thus, the proposed best estimates and ranges should be considered conservative minimum estimates of total soil CO_2 and $S(z)$ in paleosols.

5.2. Paleo-soil productivity and comparison to other soil CO_2 proxies

Non-equilibrium pairs may reflect a lack of contemporaneity between analyzed pedogenic carbonate and associated SOM, isotopic disequilibrium during carbonate precipitation, or unaccounted for substantial decay-related C isotope effects or short-term, moisture-induced changes in photosynthetic isotope fractionation (Section 4.1). The measured $\delta^{13}C$ values of soil carbonate and SOM from such non-equilibrium soils would not provide reliable estimates of soil CO_2 for application to the paleo-CO_2 barometer. That said, for paleosols that predate the evolution of C4 plants (~7–8 Ma), for which temporal change in floral composition can be considered negligible, and for which isotopic disequilibrium can be reasonably dismissed, $\Delta^{13}C$ values ($\delta^{13}C_{carb} - \delta^{13}C_{SOM}$) of >16‰ are best interpreted as a proxy of carbonate precipitation during periods of low soil productivity and thus greater penetration of atmospheric CO_2 into the soil (Stevenson et al., 2005; Sheldon and Tabor, 2009). The $\Delta^{13}C$ values of all C3 pedogenic carbonate and SOM pairs ($n = 82$) in this study's compilation of Holocene soils define a weak asymptotic correlation (r^2 of 0.31) with estimated total soil CO_2 (Fig. 6) and suggest that non-equilibrium C3 soils ($\Delta^{13}C$ of >16‰) formed in soil atmospheres of ⩽2000 ppmv; for pairs characterized by $\Delta^{13}C$ values of 18‰ or higher, soil CO_2 was likely ⩽1000 ppmv. Such values overlap the measured CO_2 range during inferred calcite precipitation in the 'non-equilibrium' grassland, shrubland, and woodland modern soils from central New Mexico (Table 2, Breecker et al., 2009).

Soil productivity and respiration rate, and in turn, soil-respired and total soil CO_2 concentrations, are governed by surface and soil temperature (Wiant, 1967a; Van Cleve and Sprague, 1971; Fang et al., 1998) and soil moisture conditions (Tamm and Kryzysch, 1963; Wiant, 1967b). Soil texture, saturation and porosity structure, including macroconduits such as in Vertisols, superimpose a local, albeit potentially large, influence on total soil CO_2 (Miotke, 1974; Breecker et al., in press). Building on the climate-soil productivity relationship, and given that mean annual precipitation (MAP) is broadly a measure of available soil moisture, it has been suggested that MAP may be a proxy of paleosol CO_2 (Cotton and Sheldon, 2012). In their study, a literature compilation of 23 modern carbonate-bearing soils documents a linear correlation (r^2 of 0.59, standard error of ±681 ppmv) between MAP and minimum summer soil CO_2 concentration. Cotton and Sheldon (2012) suggest this MAP-based proxy of soil CO_2, validated in 12 modern soils, is limited in application to paleosol analogs of Aridisols, Inceptisols, and Mollisols. If a correlation between MAP and soil CO_2 concentration is robust then $S(z)$ in paleosols can be constrained using MAP estimates inferred

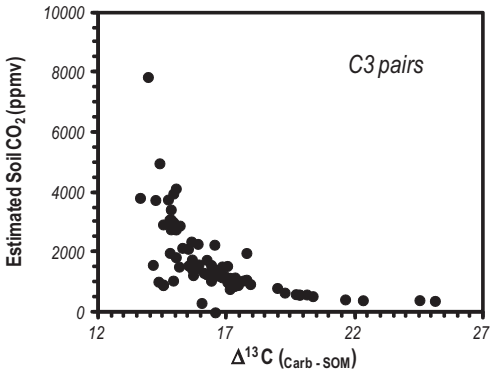

Fig. 6. Relationship between $\Delta^{13}C_{carb-SOM}$ and total soil CO_2 estimates for all C3 pairs.

from the elemental geochemistry of B horizons in paleosols (i.e., the chemical index of alteration without K, Sheldon et al., 2002), the depth to the carbonate nodular horizon (Bk) (Retallack, 2005, 2009), and for Vertisols, the calcium and magnesium oxide weathering index (Nordt and Driese, 2010).

Estimated values of soil CO_2 reported in this study for all 130 soils (233 horizons) exhibit no statistically significant correlation with MAP (r^2 of 0.02) although the mean 'best estimates' for each soil order define a weak but statistically insignificant trend (r^2 of 0.09) of increased soil CO_2 with higher MAP (Fig. 7). Moreover, no correlation between MAP and $\delta^{13}C_{carb}$ ($r^2 = 0.19$), $\Delta^{13}C$ ($r^2 = 0.07$) or $\delta^{13}C_{SOM}$ ($r^2 = 0.14$) in C3 soils was found as would be expected if soil productivity is strongly influenced by mean annual precipitation (Stevenson et al., 2005). That said, the soil CO_2 estimates derived from equilibrium and non-equilibrium pairs of Aridisols ($n = 45$) do show moderate positive correlation with MAP ($r^2 = 0.46$ and 0.61, respectively). Inceptisols show no correlation, whereas Mollisols, Alfisols and Vertisols define a weak to moderate *inverse* correlation. The moderate positive correlation defined by the Aridisols in this study, in the context of the overall lack of correlation defined by the much larger dataset and spectrum of soils, might reconcile the apparent contradictory findings of this study with those of Cotton and Sheldon (2012). The lack of clear correlation between inferred primary productivity, estimated soil CO_2, and MAP may reflect that in regions where moisture limits soil CO_2 production, characteristic of many carbonate-bearing soils, warm season soil CO_2 is more strongly correlated with actual evapotranspiration (AET) than MAP or mean annual temperature (Brook et al., 1983; Gulbranson et al., 2011b). Geographic variation in the temporal relationship between the seasonal distribution of rainfall and annual evapotranspiration predicts that soil moisture and soil CO_2 during carbonate formation likely have minimal relationship to mean annual precipitation (Gulbranson et al., 2011b and references within).

The depth to the calcic nodular horizon (Bk) in soils has been further suggested as a proxy for soil-respired CO_2 based on a significant correlation ($r^2 = 0.80$) with CO_2 contents during the late growing season (late July through early September) in 15 modern carbonate-bearing soils (Retallack, 2009). No relationship to MAP would be expected given that this period of the year would be among the wettest months in monsoonal climates and the driest in Mediterranean climates. Depth to the Bk horizon, which was defined for 46 of the soil profiles used in this study, shows no relationship with soil CO_2 estimated using equilibrium (r^2 of 0.03) and non-equilibrium pairs (r^2 of 0.02). The lack of correlation between these parameters likely reflects that soil carbonate precipitation is thermodynamically favored during the hot, driest period of the year (Breecker et al., 2009; Passey et al., 2010) rather than during mean or late growing season conditions. Moreover, this proxy has limited

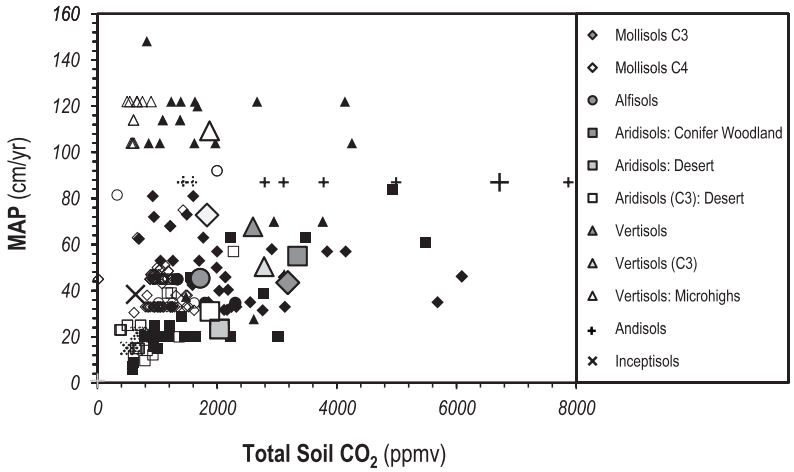

Fig. 7. Relationship between MAP and total soil CO_2 estimates. Mean estimates, by soil order, are shown by large symbols; individual equilibrium pairs (filled symbols and solid crosses and '×'s) and non-equilibrium pairs (open symbols and dashed crosses and '×'s) are plotted by soil order using similar, smaller symbols (e.g., squares for Aridisols, triangles for Vertisols). No correlation exists between MAP and soil CO_2 estimates of equilibrium pairs (r^2 of 0.02) or mean values of all soil orders (r^2 of 0.08). Data for Vertisol slopes and microlows plot off the graph. See Section 5.2 for more detail.

applicability given that the uppermost horizon(s) of soils is commonly eroded prior to burial (Cotton and Sheldon, 2012).

The two-component CO_2-mixing equation used in this study permits further constraint of estimated total and respired soil CO_2 for the paleo-CO_2 barometer. The denominator of Eq. (2) ($\delta^{13}C_{meas\ carb} - \delta^{13}C_{pred\ carb\text{-}resp\ CO2}$) approaches zero as the proportion of respired CO_2 in the soil atmosphere reaches 100%, and increases with increasing atmospheric component to total soil CO_2. A plot of these $\Delta^{13}C$ values (herein referred to as $\Delta^{13}C_{cc\ meas\text{-}pred}$) versus the best estimates of soil CO_2 for the suite of Holocene soils used in this study (Fig. 8) defines the anticipated asymptotic trend. Notably, the sharp upper boundary of this trend is delineated by the C3 soils for which the numerator ($\delta^{13}C_{pred\ carb\text{-}atm} - \delta^{13}C_{pred\ carb\text{-}resp\ CO2}$) remains relatively constant ($14‰ \pm 1‰$). This reflects the narrow range in measured $\delta^{13}C_{SOM}$ and temperatures during the warm months of decreasing or low soil moisture at each C3 site.

This C3 trend can be described by the relationship 'total soil $CO_2 = 4200/\Delta^{13}C_{cc\ meas\text{-}pred}$' indicating that total soil CO_2 under conditions of low atmospheric CO_2 (300 ppmv) is predictably related to $\Delta^{13}C$ via the dividend, 4200 (Fig. 8). For periods of higher atmospheric CO_2 and for a given set of measured $\delta^{13}C_{carb}$ and $\delta^{13}C_{SOM}$ in C3 paleosols, this dividend would scale up in proportion to the anticipated increase in atmospheric CO_2. Estimated $\Delta^{13}C_{cc\ meas\text{-}pred}$ values can therefore be used qualitatively to further constrain the portion of the proposed ranges of soil order-specific CO_2 that might best represent $S(z)$ for a given suite of spatially or temporally distributed paleosols. For a group of penecontemporaneous paleosols, variation in $\Delta^{13}C_{cc\ meas\text{-}pred}$ across sites, along with morphological or geochemical characteristics, can be used to assess *relative* differences in soil productivity and soil-respired CO_2 in the paleosol atmosphere during carbonate formation at the landscape- to global-scale. In turn, $S(z)$ input values for the paleosol-carbonate CO_2-barometer can be adjusted accordingly for site-specific subpopulations of paleosol carbonates leading to better constrained estimates. For paleosol time series, $\Delta^{13}C_{cc\ meas\text{-}pred}$ values permit evaluation of temporal change in soil moisture, in particular within morphological groupings of paleosols, that can be considered along with any independent proxy data for determining the most appropriate $S(z)$ values and for interpreting the reconstructed paleo-atmospheric CO_2. For example, the aforementioned MAP-based soil CO_2 proxy, which may have application to modern Aridisols and their paleosol analogs, could be utilized as well as an independent mechanism for refining the range of paleosol $S(z)$ estimates defined by this study.

6. SUMMARY

- Application of the $\delta^{13}C$ values of paired pedogenic carbonates and SOM from 130 Holocene soils (233 horizons) to a two-component CO_2-mixing model permits reconstruction of total and respired soil CO_2 during calcite precipitation. The carbonate–SOM pairs with $\Delta^{13}C_{carb\text{–}SOM}$ of ~12–16‰ (equilibrium pairs) constrain soil order-specific CO_2 estimates suggesting an overall range of near atmospheric to ~6000 ppmv during carbonate precipitation. Uncertainties in temperature of carbonate precipitation, decay-related and photosynthetic C isotope fractionation effects, and the potential for disequilibrium isotope fractionation delineate errors

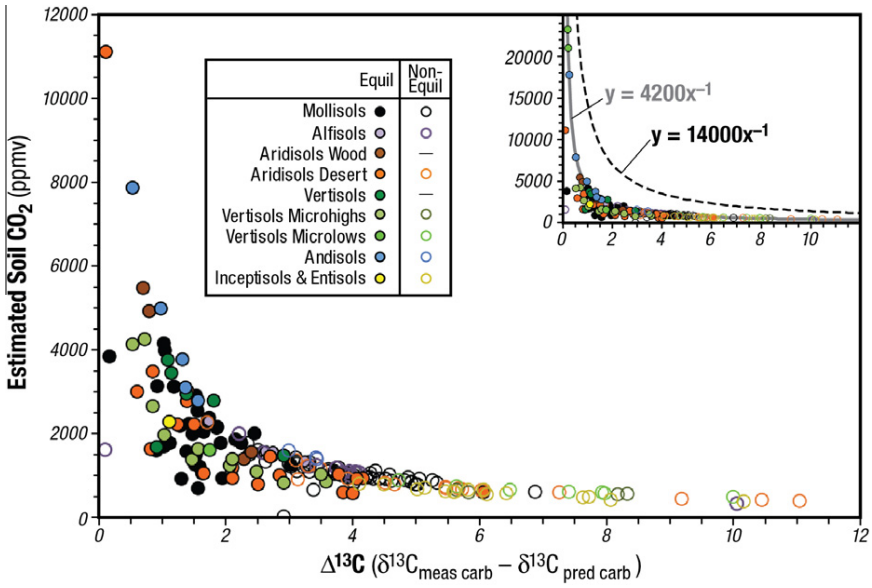

Fig. 8. Asymptotic relationship between $\Delta^{13}C_{cc\ meas\text{-}pred}$ and total soil CO_2 estimates shown by soil order for equilibrium and non-equilibrium pairs. Inset shows trends extended to 25,000 ppmv. Trend lines (power fit to the data) are for an atmospheric CO_2 content of 300 ppmv (solid curve) and 1000 ppmv (dashed curve).

of ±10–50% for soil CO_2 estimates, with the magnitude of uncertainty increasing with the magnitude of total or soil-respired CO_2. Regression analysis of equilibrium pairs indicate an effective $\Delta^{13}C$ of 14.1‰ and a mean precipitation temperature of 20 °C ± 0.6 °C. On a first-order scale, $\Delta^{13}C_{carb–SOM}$ values in C3 paleosols that exceed 16‰ can be considered indicative of total soil CO_2 concentrations of well less than 2000 ppmv.

- Soil-respired CO_2 estimates of 1500–2000 ppmv (range of ~500–2500 ppmv) for Aridisols and Alfisols (and their paleosol analogs Calcisols and Argillisols), characterized by net soil-moisture deficit, overlap the range measured in modern dryland soils during the inferred period of calcite precipitation (~700–2500 ppmv). Of these soils, those that exhibit evidence of overall higher soil moisture, productivity and/or elevation indicate soil CO_2 values of ~2000–5000 ppmv. Immature soils (Inceptisols, Entisols and their paleosol analog, Protosols) yield near atmospheric levels of total soil CO_2 (400 ± 200 ppmv). The proposed best estimates and ranges of total and respired soil CO_2 are minimum values for paleosols as they would scale upward with increasing paleo-atmospheric CO_2.
- Soil CO_2 estimates for Vertisols define the largest range (<1000 to >25,000 ppmv) reflecting their dynamic hydrochemistry likely involving calcite dissolution–precipitation cycles under fluctuating closed to open system C isotope conditions. Appropriate $S(z)$ values must distinguish between calcite precipitation in well-drained aerated soils ($S(z)$ of 2000 ± 1000 ppmv), with precipitation possibly driven by rapid degassing, from that formed in seasonally saturated soils when diffusivity between the soil and troposphere CO_2 reservoirs is limited. An upper limit for $S(z)$ of 5000 to >10,000 ppmv may best characterize paleo-Vertisols for which a net positive soil moisture regime is inferred. $\Delta^{13}C_{carb–SOM}$ values <12‰ in Vertisols likely record carbonate formation in closed, single CO_2 component systems and should not be used for paleo-atmospheric reconstructions.
- Overall lack of statistical correlation of soil CO_2 estimates with mean annual precipitation (MAP) or depth to the calcic nodular zone (Bk), likely reflects that for regions where moisture limits soil CO_2 production, relevant to many carbonate-bearing soils, soil CO_2 is more strongly correlated with actual evapotranspiration than with MAP or mean annual temperature. A possible exception for Aridisols may exist but requires further evaluation.
- $\Delta^{13}C$ ($\delta^{13}C_{meas\ carb} - \delta^{13}C_{pred\ carb\text{-}soilresp\ CO2}$) values for paleosols provide a spatial or temporal record of relative variation in soil productivity and, in turn, total and respired soil CO_2, and when considered within the context of paleosol morphology, structure and texture can be used to refine the proposed estimates of soil CO_2 for reconstruction of paleo-atmospheric pCO_2.

ACKNOWLEDGMENTS

Irina Kovda, Neil Tabor and Jason Mintz are acknowledged for graciously sharing data, information about climate and soil conditions at specific sites, and for fruitful discussions regarding efforts to constrain soil CO_2 for paleosol-based reconstruction of past atmospheric CO_2. Neil Kelley and Jessica Oster provided assistance with the statistical analysis. Steve Driese and Dana Royer are acknowledged for their thoughtful and very constructive reviews. This research was supported by NSF Grant EAR-1024737 and a Fellowship from the John Simon Guggenheim Foundation.

APPENDIX A. SUPPLEMENTARY DATA

Supplementary data associated with this article can be found, in the online version, at http://dx.doi.org/10.1016/j.gca.2012.10.012.

REFERENCES

Amundson R. G. and Davidson E. A. (1990) Carbon dioxide and nitrogenous gases in the soil atmosphere. *J. Geochem. Explor.* **38**, 13–41.

Amundson R. G., Chadwick O. A., Sowers J. and Doner H. E. (1988) The relationship between modern climate and vegetation and the stable isotope chemistry of Mojave Desert soils. *Quatern. Res.* **29**, 245–254.

Amundson R. G. (1989) The stable isotope chemistry of pedogenic carbonates at Kyle Canyon, Nevada. *Soil Sci. Soc. Am. J.* **53**, 201–210.

Amundson R. G., Franco-Vizcaino E., Graham R. C. and DeNiro M. (1994) The relationship of precipitation seasonality to the flora and stable isotope chemistry of soils in the Vizcaino desert, Baja California, Mexico. *J. Arid Environ.* **28**, 265–279.

Arens N. C., Jahren A. H. and Amundson R. (2000) Can C3 plants faithfully record the carbon isotopic composition of atmospheric carbon dioxide?. *Paleobiology* **26** 137–164.

Beerling D. J. and Royer D. L. (2011) Convergent Cenozoic CO_2 history. *Nat. Geosci.* **4**, 418–420.

Berner R. A. (1997) The rise of land plants and their effects on weathering and atmospheric CO_2. *Science* **276**, 543–546.

Berner R. A. (2006) GEOCARBSULF; a combined model for Phanerozoic atmospheric O_2 and CO_2. *Geochim. Cosmochim. Acta* **70**, 5653–5664.

Bowen G. J. and Beerling D. J. (2004) An integrated model for soil organic carbon and CO_2: implications for paleosol carbonate pCO_2 paleobarometry. *Global Biogeochem. Cycles* **18**, GB1026. http://dx.doi.org/10.1029/2003GB002117.

Breecker D. O., Sharp Z. D. and McFadden L. D. (2009) Seasonal bias in the formation and stable isotopic composition of pedogenic carbonate in modern soils from central New Mexico, USA. *Geol. Soc. Am. Bull.* **121**, 630–640.

Breecker D. O., Yoon J., Michel L. A., Dinka T. M., Driese S. G., Mintz J. S., Nordt L. C., Romanak K. D. and Morgan C. L. S. (in press) CO_2 concentrations in Vertisols: seasonal variability and shrink-swell. In *New Frontiers in Paleopedology and Terrestrial Paleoclimatology* (eds. S. G. Driese and L. C. Nordt.). SEPM Spec. Pub., Tulsa, OK.

Brook G. A., Folkoff M. E. and Box E. O. (1983) A world model of soil carbon dioxide. *Earth Surf. Proc. Land.* **8**, 79–88.

Buck B. J. and Monger H. C. (1999) Stable isotopes and soil–geomorphology as indicators of Holocene climate change, northern Chihuahuan Desert. *J. Arid Environ.* **43**, 357–373.

Buol S. W., Southard R. J., Graham R. C. and McDaniel P. A. (2003) *Soil Genesis and Classification*, fifth ed. Iowa St. Press, Ames, Iowa, USA, 494p.

Cerling T. E. (1984) The stable isotopic composition of modern soil carbonate and its relationships to climate. *Earth Planet. Sci. Lett.* **71**, 229–240.

Cerling T. E. (1991) Carbon dioxide in the atmosphere: evidence from Cenozoic and Mesozoic paleosols. *Am. J. Sci.* **291**, 377–400.

Cerling T. E. (1999) Stable carbon isotopes in paleosol carbonates. In *Palaeoweathering, Palaeosurfaces, and Related Continental Deposits* (eds. M. Thirty and R. Coincon). Int. Assoc. Sediment. Spec. Pub. **27**. Oxford Press, Oxford, UK, pp. 43–60.

Cerling T. E. and Quade J. (1993) Stable carbon and oxygen isotopes in soil carbonates. In *Climate Change in Continental Isotopic Records* (eds. J. A. McKenzie and S. Savin). Geophysical Monograph **78**. American Geophysical Union, Washington, DC, pp. 217–231.

Cerling T. E., Solomon D. K., Quade J. and Bowman J. R. (1991) On the isotopic composition of carbon in soil carbon dioxide. *Geochim. Cosmochim. Acta* **55**, 3403–3405.

Cleveland D. M., Nordt L. C., Dworkin S. I. and Atchley S. C. (2008) Pedogenic carbonate isotopes as evidence for extreme climatic events preceding the Triassic–Jurassic boundary: implications for the biotic crisis?. *Geol. Soc. Am. Bull.* **120** 1408–1415.

Cotton J. M. and Sheldon N. D. (2012) New constraints on using paleosols to reconstruct atmospheric CO_2. *Geol. Soc. Am. Bull.* **124**, 1411–1423. http://dx.doi.org/10.1130/B30607.1.

Davidson G. R. (1995) The stable isotopic composition and measurement of carbon in soil CO_2. *Geochim. Cosmochim. Acta* **59**, 2485–2489.

Deutz P., Montañez I. P., Monger H. C. and Morrison J. (2001) Morphology and isotope heterogeneity of Late Quaternary pedogenic carbonates: implications for paleosol carbonates as paleoenvironmental proxies. *Palaeogeogr. Palaeoclimatol. Palaeoecol.* **166**, 293–317.

Deutz P., Montañez I. P. and Monger H. C. (2002) Morphologies and stable and radiogenic isotope compositions of pedogenic carbonates in Late Quaternary relict and buried soils, New Mexico: an integrated record of pedogenic overprinting. *J. Sediment. Res.* **72**, 809–822.

Driese S. G., Mora C. I. and Elick J. M. (2000) The paleosol record of increasing plant diversity and depth of rooting and changes in atmospheric pCO_2 in the Siluro-Devonian. In *Phanerozoic Terrestrial Ecosystems* (ed. R. D. White). Paleontol. Soc. Spec. Pub. **6**, New Haven, pp. 47–61.

Ekart D. D., Cerling T. E., Montañez I. P. and Tabor N. J. (1999) A 400 million year carbon isotope record of pedogenic carbonate: implications for paleoatmospheric carbon dioxide. *Am. J. Sci.* **299**, 805–827.

Fang C., Moncrieff J. B., Gholz H. L. and Clark K. L. (1998) Soil CO_2 efflux and its spatial variation in a Florida Slash pin plantation. *Plant Soil* **205**, 135–146.

Farquhar G. D., Ehleringer J. R. and Hubick K. T. (1989) Carbon isotope discrimination and photosynthesis. *Annu. Rev. Plant Physiol. Plant Mol. Biol.* **40**, 503–537.

Francey R. J., Allison C. E., Etheridge D. M., Trudinger C. M., Enting I. G., Leuenberger M., Langenfelds R. L., Michel E. and Steele L. P. (1999) A 1000 year high precision record of $\delta^{13}C$ in atmospheric CO_2. *Tellus Ser. B* **51B**, 170–193.

Ghosh P., Ghosh P. and Bhattacharya S. K. (2001) CO_2 levels in the Late Palaeozoic and Mesozoic atmosphere from soil carbonate and organic matter, Satpura basin, Central India. *Palaeogeogr. Palaeoclimatol. Palaeoecol.* **170**, 219–236.

Gröcke D. R. (2002) The carbon isotope composition of ancient CO_2 based on higher plant organic matter. In *Understanding Climate Change: Proxies, Chronology, and Ocean–Atmosphere Interactions*, vol. 360 (eds. D. R. Gröcke and M. Kucera). Royal Society, London, pp. 633–658.

Grossman E. L., Yancey T. E., Jones T. E., Bruckschen P. and Chuvashov B., et al. (2008) Glaciation, aridification, and carbon sequestration in the Permo-Carboniferous: the isotopic record from low latitudes. *Palaeogeogr. Palaeoclimatol. Palaeoecol.* **268**, 222–233.

Gulbranson E. L., Tabor N. J. and Montañez I. P. (2011a) Response of soil CO_2 to variations in soil moisture content recorded in paleosol goethite. *Geochim. Cosmochim. Acta* **75**, 7099–7116.

Gulbranson E. L., Montañez I. P. and Tabor N. J. (2011b) A proxy for humidity and floral province from paleosols. *J. Geol.* **119**, 559–573.

Hansen J., Sato M., Kharecha P., Beerling D., Berner R., Masson-Delmotte V., Pagani M., Raymo M., Royer D. L. and Zachos J. C. (2008) Target atmospheric CO_2: where should humanity aim? *Open Atmos. Sci. J.* **2**, 217–231. http://dx.doi.org/10.2174/1874282300802010217.

Haywood A. M., Ridgwell A., Lunt D. J., Hill M. J., Pound J., Dowsett H. J., Dolan A. M., Francis J. E. and Williams M. (2011) Are there pre-Quaternary geological analogues for a future greenhouse warming? *Philos. Trans. R. Soc. A* **369**, 933–956.

Honisch B., Ridgwell A. and Schmidt D. N., et al. (2012) The geological record of ocean acidification. *Science* **335**, 1058–1063.

IPCC (2007) Climate change 2007: the physical science basis. In *Contribution of Working Group I to the Fourth Assessment Report of the Intergovernmental Panel on Climate Change* (eds. S. Solomon, D. Qin, M. Manning, Z. Chen, M. Marquis, K. B. Averyt, M. Tignor and H. L. Miller). Cambridge University Press, Cambridge, 996p.

Kelly E. F., Amundson R. G., Marino B. D. and DeNiro M. J. (1991) Stable carbon isotopic composition of carbonate in Holocene grassland soils. *Soil Sci. Soc. Am. J.* **55**, 1651–1658.

Kidder D. L. and Worsley T. R. (2012) A human-induced hothouse climate? *GSA Today* **22**, 4–11.

Kovda I., Mora C. I. and Wilding L. P. (2006) Stable isotope compositions of pedogenic carbonates and soil organic matter in a temperate climate Vertisol with gilgai, southern Russia. *Geoderma* **136**, 423–435.

Knutti R. and Hegerl G. C. (2008) The equilibrium sensitivity of the earth's temperature to radiation changes. *Nat. Geosci.* **1**, 735–743.

Landi A. (2002) Carbon balance in major soil zones in Saskatchewan. Ph.D. thesis, Univ. Saskatchewan, Saskatoon, Canada.

Landi A., Mermut A. R. and Anderson D. W. (2003) Origin and rate of pedogenic carbonate accumulation in Saskatchewan soils, Canada. *Geoderma* **117**, 143–156.

Laskar A. H., Sharma N., Ramesh R., Jani R. A. and Yadava M. G. (2010) Paleoclimate and paleovegetation of Lower Narmada Basin, Gujarat, Western India, inferred from stable carbon and oxygen isotopes. *Quatern. Int.* **227**, 183–189.

Machette M. N. (1985) Calcic soils of the southwestern United States. *Geol. Soc. Am. Spec. Paper* **203**, 1–22.

Mack G. H., James W. C. and Monger H. C. (1993) Classification of paleosols. *Geol. Soc. Am. Bull.* **105**, 129–136.

Matsumoto E., Naruoka T. and da Silva E. F. (1997) Concentration of carbon dioxide in regolith air in different tropical geoecosystems of northeast Brazil. *Inst. Geosci. Univ. Tsukuba Annu. Rept.* **23**, 11–15.

Miller D. L. (2000) Occurrence and stable isotope compositions of soil carbonate and organic matter within a climatic transect of modern Vertisols along the Coastal Prairie of Texas. M.S. thesis, Univ. of Tenn., Knoxville.

Miller D. L., Mora C. I. and Driese S. G. (2007) Isotopic variability in large carbonate nodules in Vertisols: implications for climate and ecosystem assessments. *Geoderma* **142**, 104–111.

Mintz J. S., Driese S. G., Breecker D. O. and Ludvigson G. A. (2011) Influence of changing hydrology on pedogenic calcite precipitation in Vertisols, Dance Bayou, Brazoria County, Texas, USA: implications for estimating paleoatmospheric pCO_2. *J. Sediment. Res.* **81**, 394–400.

Miotke F.-D. (1974) Carbon dioxide and the soil atmosphere. *Abh. Karst – Hohlenkunde Ser. A* **9**, 1–49.

Monger H. C., Cole D. R., Gish J. W. and Giordana T. H. (1998) Stable carbon and oxygen isotopes in Quaternary soil carbonates as indicators of ecogeomorphic changes in the northern Chihuahuan Desert, USA. *Geoderma* **82**, 137–172.

Montañez I. P., Tabor N. J., Niemeier D., DiMichele W. A., Frank T. D., Fielding C. R., Isbell J. L., Birgenheier L. P. and Rygel M. C. (2007) CO_2-forced climate and vegetation instability during Late Paleozoic deglaciation. *Science* **315**, 87–91.

Mora C. I., Driese S. G. and Colarusso L. A. (1996) Middle and Late Paleozoic atmospheric CO_2 levels from soil carbonate and organic matter. *Science* **271**, 1105–1107.

Nadelhoffer K. J. and Fry B. (1988) Controls on natural Nitrogen-15 and Carbon-13 abundances in forest soil organic matter. *Soil Sci. Soc. Am. J.* **52**, 1633–1640.

NRC Committee on the Importance of Deep-Time Geologic Records for Understanding Climate Change Impacts (Montañez I. P., Chair) (2011) *Understanding Earth's Deep Past: Lessons for Our Climate Future*. National Academies Press, Washington, DC, 161p.

Nordt L. and Driese S. D. (2010) New weathering index improves paleorainfall estimates from Vertisols. *Geology* **38**, 407–410.

Nordt L., Atchley S. and Dworkin S. I. (2002) Paleosol barometer indicates extreme fluctuations in atmospheric CO_2 across the Cretaceous–Tertiary boundary. *Geology* **30**, 703–706.

Nordt L. (2003) Terrestrial evidence for two greenhouse events in the latest Cretaceous. *GSA Today* **13**, 4–9.

Nordt L., Orosz M., Driese S. and Tubbs J. (2006) Vertisol carbonate properties in relation to mean annual precipitation: implications for paleoprecipitation estimates. *J. Geol.* **114**, 501–510.

Parker L. W., Miller J., Steinberger Y. and Whitford W. G. (1983) Soil respiration in a Chihuahuan desert rangeland. *Soil Biol. Biochem.* **15**, 303–309.

Passey B. H., Levin N. E., Cerling T. E., Brown F. H. and Eiler J. M. (2010) High- temperature environments of human evolution in East Africa based on bond ordering in paleosol carbonates. *Proc. Natl. Acad. Sci. USA* **107**, 11245–11249.

Pendall E. and Amundson R. D. (1990) The stable isotope chemistry of pedogenic carbonate in an alluvial soil from the Punjab, Pakistan. *Soil Sci.* **149**, 199–211.

Pendall E. G., Harden J. W., Trumbore S. E. and Chadwick O. A. (1994) Isotopic approach to soil carbonate dynamics and implication for palaeoclimatic interpretations. *Quatern. Res.* **42**, 60–71.

Prasad V., Stroemberg C. A., Alimohammadian H. and Sahni A. (2005) Dinosaur coprolites and the early evolution of grasses and grazers. *Science* **310**, 1177–1180.

Prochnow S. J., Nordt L. C., Atchley S. C. and Hudec M. R. (2006) Multi-proxy paleosol evidence for middle and late Triassic climate trends in eastern Utah. *Palaeogeogr. Palaeoclimatol. Palaeoecol.* **232**, 53–72.

Prokoph A., Shields G. A. and Veizer J. (2008) Compilation and time-series analysis of a marine carbonate $\delta^{18}O$, $\delta^{13}C$, $^{87}Sr/^{86}Sr$ and $\delta^{34}S$ database through Earth history. *Earth-Sci. Rev.* **87**, 113–133.

Quade J., Cerling T. E. and Bowman J. R. (1989) Systematic variations in the carbon and oxygen isotopic composition of pedogenic carbonate along elevation transects in the southern Great Basin, United States. *Geol. Soc. Am. Bull.* **101**, 464–475.

Quade J., Breecker D. O., Daeron M. and Eiler J. (2011) The paleoaltimetry of Tibet: an isotopic perspective. *Am. J. Sci.* **311**, 77–115.

Rabenhorst M. C., Wilding L. P. and West L. T. (1984) Identification of pedogenic carbonates using stable carbon isotope and microfabric analysis. *Soil Sci. Soc. Am.* **48**, 125–132.

Retallack G. J. (2005) Pedogenic carbonate proxies for amount and seasonality of precipitation in paleosols. *Geology* **33**, 333–336.

Retallack G. J. (2009) Refining a pedogenic-carbonate CO_2 paleobarometer to quantify a middle Miocene greenhouse spike. *Palaeogeogr. Palaeoclimatol. Palaeoecol.* **281**, 57–65.

Robinson S. A., Andrews J. E., Hesselbo S. P., Radley J. D., Dennis P. F., Harding I. C. and Allen P. (2002) Atmospheric pCO_2 and depositional environment from stable-isotope geochemistry of calcrete nodules (Barremian, Lower Cretaceous, Wealden Beds, England). *J. Geol. Soc. Lond.* **159**, 215–224.

Romanek C. S., Grossman E. L. and Morse J. W. (1992) Carbon isotopic fractionation in synthetic aragonite and calcite: effects of temperature and precipitation rate. *Geochim. Cosmochim. Acta* **56**, 419–430.

Rovira P. and Vallejo V. R. (2008) Changes in $\delta^{13}C$ composition of soil carbonates driven by organic matter decomposition in a Mediterranean climate: a field incubation experiment. *Geoderma* **144**, 517–534.

Royer D. L., Berner R. A. and Beerling D. J. (2001) Phanerozoic atmospheric CO_2 change: evaluating geochemical and paleobiological approaches. *Earth-Sci. Rev.* **54**, 349–392.

Salehi M. H., Khademi H., Eghbal M. K. and Mermut A. R. (2004) Stable isotope geochemistry of carbonates and organic carbon in selected soils from Chaharmahal Bakhtiari Province, Iran. *Commun. Soil Sci. Plant Anal.* **35**, 1681–1697.

Santruckova H., Bird M. I. and Lloyd J. (2000) Microbial processes and carbon-isotope fractionation in tropical and temperate grassland soils. *Funct. Ecol.* **14**, 108–114.

Schaller M. F., Wright J. D. and Kent D. V. (2011) Atmospheric pCO_2 perturbations associated with the Central Atlantic Magmatic Province. *Science* **331**, 1404–1409.

Sheldon N. D. and Tabor N. J. (2009) Quantitative paleoenvironmental and paleoclimatic reconstruction using paleosols. *Earth-Sci. Rev.* **95**, 1–52.

Sheldon N. D., Retallack G. J. and Tanaka S. (2002) Geochemical climofunctions from North America soils and application to paleosols across the Eocene–Oligocene boundary in Oregon. *J. Geol.* **110**, 687–696.

Serna-Perez A., Monger H. C., Herrick J. E. and Murray L. (2006) Carbon dioxide emissions from exhumed petrocalcic horizons. *Soil Sci. Soc. Am. J.* **70**, 795–805.

Siegenthaler U., Stocker T. F., Monnin E., Luthi D., Schwander J., Stauffer B., Raynaud D., Barnola J.-M., Fischer H., Masson-Delmotte V. and Jouzel J. (2005) Stable carbon cycle–climate relationship during the late Pleistocene. *Science* **310**, 1313–1317.

Soil Survey Staff (2010) *Keys to Soil Taxonomy*, 11th ed. US Department of Agriculture, Natural Resources Conservation Service, Washington, DC, 346 pp.

Soloman D. K. and Cerling T. E. (1987) The annual carbon dioxide cycle in a montane soil: observations, modeling, and implications for weathering. *Water Resour. Res.* **23**, 2257–2265.

Stevenson B. A., Kelly E. F., McDonald E. V. and Busacca A. J. (2005) The stable carbon isotope composition of soil organic carbon and pedogenic carbonates along a bioclimatic gradient in the Palouse region, Washington State, USA. *Geoderma* **124**, 37–47.

Tabor N. J., Meyers T. S., Gulbranson E. L., Rasmussen C. and Sheldon N. (in press) Carbon stable isotope composition of modern calcareous soil profiles in California: implications for CO_2 reconstructions from calcareous paleosols. In *New Frontiers in Paleopedology and Terrestrial Paleoclimatology* (eds. S. G. Driese and L. C. Nordt.). SEPM Spec. Pub., Tulsa, OK.

Tanner L. H., Hubert J. F., Coffey B. P. and McInerney D. P. (2001) Stability of atmospheric CO_2 levels across the Triassic/Jurassic boundary. *Nature* **411**, 675–677.

Van Cleve K. and Sprague D. (1971) Respiration rates in the forest floor of birch and aspen stands in interior Alaska. *Arctic Alpine Res.* **3**, 17–26.

Veizer J., Ala D., Azmy K., Bruckschen P., Buhl D., Bruhn F., Carden G. A. F., Diener A., Ebneth S., Godderis Y., Jasper T., Korte C., Pawellek F., Podhaha O. G. and Strauss H. (1999) $^{87}Sr/^{86}Sr$, $\delta^{13}C$, and $\delta^{18}O$ evolution of Phanerozoic seawater. *Chem. Geol.* **161**, 59–88.

Wang D. and Anderson D. W. (1998) Stable carbon isotopes of carbonate pendants from Chernozemic soils of Saskatchewan, Canada. *Geoderma* **84**, 309–322.

Wang Y., Cerling T. E. and Effland W. R. (1993) Stable isotope ratios of soil carbonate and soil organic matter as indicators of forest invasion of prairie near Ames, Iowa. *Oecologia* **95**, 365–369.

Wang Y., McDonald E., Amundson R., McFadden L. and Chadwick O. (1996) An isotopic study of soils in chronological sequences of alluvial deposits, Providence Mountains, California. *Geol. Soc. Am. Bull.* **108**, 379–391.

Wedin D. A., Tieszen L. L., Dewey B. and Pastor J. (1995) Carbon-isotope dynamics during grass decomposition and soil organic-matter formation. *Ecology* **76**, 1383–1392.

Wiant H. V. (1967a) Influence of temperature on the rate of soil respiration. *J. Forest.* **65**, 489–490.

Wiant H. V. (1967b) Influence of moisture content on 'soil respiration'. *J. Forest.* **65**, 902–903.

Yapp C. J. and Poths H. (1996) Carbon isotopes in continental weathering environments and variations in ancient atmospheric CO_2 pressure. *Earth Planet. Sci. Lett.* **137**, 71–82.

Zanchetta G., Di Vito M., Fallick A. E. and Sulpizio R. (2000) Stable isotopes of pedogenic carbonates from the Somma-Vesuvius area, southern Italy, over the past 18 kyr: palaeoclimatic implications. *J. Quatern. Sci.* **15**, 813–824.

Zhang J., Quay P. D. and Wilbur D. O. (1995) Carbon-isotope fractionation during gas–water exchange and dissolution of CO_2. *Geochim. Cosmochim. Acta* **59**, 107–114.

Associate editor: Peter Hernes